On Polarization Properties of Light, Gaussian Beams and Spin-Orbit Interaction of Light.

A report submitted in fulfilment of the Summer Internship
by

Pritish Karmakar
Roll: 21MS179
BS-MS, IISER Kolkata

under

Prof. Ayan Banarjee
Department of Physical Sciences
IISER Kolkata

dated

17.05.23 - 20.07.23

Indian Institution of Science Education & Research
Kolkata, WB, India, 741246

Declaration

I, Pritish Karmakar, hereby declare that the summer internship report titled *"On Polarization Properties of Light, Gaussian Beams and Spin-Orbit Interaction of Light"* is undertaken by me as a part of the Summer Internship under Prof. Ayan Banerjee at Indian Institute of Science Education & Research, Kolkata from 17.05.23 to 20.07.23.

I affirm that the content of this report is based on my reading, research, and comprehension of the materials provided or recommended by my internship supervisor or my mentor and all the information, quotations, or ideas taken from external sources have been duly acknowledged and cited using the appropriate referencing style.

I hereby submit this report in fulfilment of this summer internship and for further evaluation and assessment.

Sincerely,
Pritish Karmakar

Acknowledgement

I am incredibly grateful to have had the opportunity to work on a fascinating summer project on the topic of optics under Prof. Ayan Banerjee[1] and with the mentorship of Ram Nandan Kumar[2]. This project has been an enriching and enlightening experience for me to deepen my understanding of the subject matter, and I am indebted to the support, encouragement and expertise provided by both of them.

I want to thank my family and my friends for their unwavering support and understanding throughout this journey. Their encouragement provided the motivation I needed to stay focused and determined. Additionally, I am grateful to the other authors on the subject whose work I utilized for assistance.

In conclusion, I feel immensely fortunate to have worked on this summer project and the knowledge and experiences gained during this period will undoubtedly shape my academic and professional pursuits in the future.

Thank you all for being an integral part of this enriching journey.

Sincerely,
Pritish Karmakar

[1]HOD, Department of Physical Sciences, IISER Kolkata, Room No: M-130, email: ayan@iiserkol.ac.in
[2]Int. PhD, Department of Physical Sciences, IISER Kolkata, email: ramnandan899@gmail.com

Contents

List of Figures

List of Tables

1 POLARIZATION

1.1 Introduction

We know, in EM wave, the electric field and magnetic field oscillating perpendicularly in the transverse plane *w.r.t.* the propagation direction. *Polarization* is the property of an EM wave, which deals with the temporal and spatial variation of the orientation of field vector (mainly, electric field) of the EM wave. Here we mainly discuss Jones formalism, Stokes-Muller formalism and finally apply those thing in elliptically polarized light.

1.2 Jones formalism

1.2.1 Jones Vector

Vector form of electric field of fully polarized EM wave propagating along z-axis is given by

$$\boldsymbol{E}(\boldsymbol{x},t) = \begin{bmatrix} E_x(\boldsymbol{x},t) \\ E_y(\boldsymbol{x},t) \\ E_z(\boldsymbol{x},t) \end{bmatrix} = \begin{bmatrix} A_x(\boldsymbol{x})e^{-i(kz-\omega t-\delta_x)} \\ A_y(\boldsymbol{x})e^{-i(kz-\omega t-\delta_y)} \\ 0 \end{bmatrix} = \begin{bmatrix} A_x(\boldsymbol{x})e^{i\delta_x} \\ A_y(\boldsymbol{x})e^{i\delta_y} \\ 0 \end{bmatrix} e^{-i(kz-\omega t)} \tag{1.1}$$

We define normalized[3] *Jones vector* as

$$\boldsymbol{J}(\boldsymbol{x},t) = \frac{1}{\sqrt{A_x^2 + A_y^2}} \begin{bmatrix} A_x(\boldsymbol{x})e^{i\delta_x} \\ A_y(\boldsymbol{x})e^{i\delta_y} \end{bmatrix} \tag{1.2}$$

Such examples of usual polarization states are given below [3],

Polarization state	$\boldsymbol{J}$
$\lvert H\rangle$	$\begin{bmatrix} 1 \\ 0 \end{bmatrix}$
$\lvert V\rangle$	$\begin{bmatrix} 0 \\ 1 \end{bmatrix}$
$\lvert P\rangle$	$\frac{1}{\sqrt{2}}\begin{bmatrix} 1 \\ 1 \end{bmatrix}$
$\lvert M\rangle$	$\frac{1}{\sqrt{2}}\begin{bmatrix} 1 \\ -1 \end{bmatrix}$
$\lvert L\rangle$	$\frac{1}{\sqrt{2}}\begin{bmatrix} 1 \\ i \end{bmatrix}$
$\lvert R\rangle$	$\frac{1}{\sqrt{2}}\begin{bmatrix} 1 \\ -i \end{bmatrix}$

Table 1: Jones vector of usual polarization state

Some properties of Jones vector are

[3] normalized as $\boldsymbol{J}^* \boldsymbol{J} = 1$

1. The intensity of the EM wave is given by

$$I = \frac{1}{2}c\epsilon_0(A_x^2 + A_y^2) = \frac{1}{2}c\epsilon_0(\boldsymbol{E}^*\boldsymbol{E}) = \frac{1}{2}c\epsilon_0(\boldsymbol{J}^*\boldsymbol{J}) \tag{1.3}$$

2. For general elliptically polarized light we can measure the azimuth (α) ellipticity (ϵ) of the polarization ellipse by comparing Jones vector $\boldsymbol{J}$ with [1]

$$\begin{bmatrix} \cos\alpha\cos\epsilon - i\sin\alpha\sin\epsilon \\ \sin\alpha\cos\epsilon + i\cos\alpha\sin\epsilon \end{bmatrix}$$

1.2.2 Jones Matrix & evolution of Jones vector

Jones matrix is a 2×2 matrix assigned for a particular optical element. Let $\boldsymbol{M}$ be the Jones matrix for an optical element *s.t.*

$$\boldsymbol{M} = \begin{bmatrix} m_{11} & m_{12} \\ m_{21} & m_{22} \end{bmatrix}$$

then if a polarized light of Jones vector $\boldsymbol{J}_{in}$ passes through that optical element then the Jones vector of output light is given by

$$\boldsymbol{J}_{out} = \boldsymbol{M}\ \boldsymbol{J}_{in} \tag{1.4}$$

$$\Rightarrow \boldsymbol{E}_{out} = \boldsymbol{M}\ \boldsymbol{E}_{in} \tag{1.5}$$

To determine m_{ij} in $\boldsymbol{M}$,

1. Pass x-polarized light and determine $\boldsymbol{J}_{out}$, then

$$\boldsymbol{J}_{out} = \begin{bmatrix} m_{11} & m_{12} \\ m_{21} & m_{22} \end{bmatrix} \begin{bmatrix} 1 \\ 0 \end{bmatrix} = \begin{bmatrix} m_{11} \\ m_{21} \end{bmatrix}$$

2. Pass y-polarized light and determine $\boldsymbol{J}_{out}$, then

$$\boldsymbol{J}_{out} = \begin{bmatrix} m_{11} & m_{12} \\ m_{21} & m_{22} \end{bmatrix} \begin{bmatrix} 0 \\ 1 \end{bmatrix} = \begin{bmatrix} m_{12} \\ m_{22} \end{bmatrix}$$

Such examples of usual Jones matrix [4] are given below,[3]

Optical element	$\boldsymbol{M}$
Free space	$\begin{bmatrix} 1 & 0 \\ 0 & 1 \end{bmatrix}$
x-polarizer	$\begin{bmatrix} 1 & 0 \\ 0 & 0 \end{bmatrix}$
y-polarizer	$\begin{bmatrix} 0 & 0 \\ 0 & 1 \end{bmatrix}$

[4] For polarizer the Jones matrix $\boldsymbol{M} = \boldsymbol{J}\ \boldsymbol{J}^*$ where $\boldsymbol{J}$ is normalized Jones vector corresponding polarization state *s.t.* $\boldsymbol{J}_{out} = \boldsymbol{M}\boldsymbol{J} = (\boldsymbol{J}\boldsymbol{J}^*)\boldsymbol{J} = \boldsymbol{J}(\boldsymbol{J}^*\boldsymbol{J}) = \boldsymbol{J}$

Optical element	$\boldsymbol{M}$
Right circular polarizer	$\frac{1}{2}\begin{bmatrix}1 & i\\ -i & 1\end{bmatrix}$
Left circular polarizer	$\frac{1}{2}\begin{bmatrix}1 & -i\\ i & 1\end{bmatrix}$
Linear di-attenuator	$\begin{bmatrix}a & 0\\ 0 & b\end{bmatrix}$
Half-wave plate with fast axis horizontal	$e^{-i\pi/2}\begin{bmatrix}1 & 0\\ 0 & -1\end{bmatrix}$
Quarter-wave plate with fast axis horizontal	$e^{-i\pi/4}\begin{bmatrix}1 & 0\\ 0 & i\end{bmatrix}$
General phase retarder	$\begin{bmatrix}e^{i\phi_x} & 0\\ 0 & e^{i\phi_y}\end{bmatrix}$

Table 2: Jones matrix related to usual optical element

Some properties of Jones matrix are

1. Resultant Jones matrix for composition of n optical elements is given by

$$\boldsymbol{M} = \boldsymbol{M}_1\,\boldsymbol{M}_2 \ldots \boldsymbol{M}_n \tag{1.6}$$

2. For an optical element when its optical axis aligned at an angle θ *w.r.t.* x-axis then resultant Jones matrix for this rotated optical element is given by

$$\boldsymbol{M}_\theta = R(-\theta)\;\boldsymbol{M}\;R(\theta) \tag{1.7}$$

   where $R(\theta)$ is passive rotation matrix *s.t.*

$$R(\theta) = \begin{bmatrix}\cos\theta & \sin\theta\\ -\sin\theta & \cos\theta\end{bmatrix} \tag{1.8}$$

1.2.3 Drawback of Jones formalism

Main drawback of Jones formalism is that its application is restricted in fully polarized light. This formalism cannot explain the partially polarized or unpolished light which we frequently observe in practical use.

1.3 Stokes-Muller formalism

1.3.1 Coherency matrix

Coherency matrix of a EM wave is defined as [1]

$$\boldsymbol{C} = \left\langle \boldsymbol{E} \otimes \boldsymbol{E}^\dagger \right\rangle = \left\langle \boldsymbol{E}\boldsymbol{E}^\dagger \right\rangle = \begin{bmatrix}\langle E_x E_x^* \rangle & \langle E_x E_y^* \rangle\\ \langle E_y E_x^* \rangle & \langle E_y E_y^* \rangle\end{bmatrix} = \begin{bmatrix}c_{xx} & c_{xy}\\ c_{yx} & c_{yy}\end{bmatrix} \tag{1.9}$$

where $\otimes$ denotes Kronecker product and $\langle\cdot\rangle$ denotes the temporal avg of the corresponding quantity.

Examples of coherency matrix of usual polarization states are given below [4],

Polarization state	$\boldsymbol{J}$	$\boldsymbol{C}$
$\lvert H\rangle$	$\begin{bmatrix}1\\0\end{bmatrix}$	$\begin{bmatrix}1&0\\0&0\end{bmatrix}$
$\lvert V\rangle$	$\begin{bmatrix}0\\1\end{bmatrix}$	$\begin{bmatrix}0&0\\0&1\end{bmatrix}$
$\lvert P\rangle$	$\frac{1}{\sqrt{2}}\begin{bmatrix}1\\1\end{bmatrix}$	$\frac{1}{2}\begin{bmatrix}1&1\\1&1\end{bmatrix}$
$\lvert M\rangle$	$\frac{1}{\sqrt{2}}\begin{bmatrix}1\\-1\end{bmatrix}$	$\frac{1}{2}\begin{bmatrix}1&-1\\-1&1\end{bmatrix}$
$\lvert L\rangle$	$\frac{1}{\sqrt{2}}\begin{bmatrix}1\\i\end{bmatrix}$	$\frac{1}{2}\begin{bmatrix}1&-i\\i&1\end{bmatrix}$
$\lvert R\rangle$	$\frac{1}{\sqrt{2}}\begin{bmatrix}1\\-i\end{bmatrix}$	$\frac{1}{2}\begin{bmatrix}1&i\\-i&1\end{bmatrix}$
Un-polarized	–	$\frac{1}{2}\begin{bmatrix}1&0\\0&1\end{bmatrix}$

Table 3: Coherency matrix of usual polarization state

Some properties of coherency matrix are

1. It is a hermitian matrix *i.e.* $\boldsymbol{C} = \boldsymbol{C}^\dagger$
2. Trace and determinant off the matrix are non-negative *i.e.* $\mathrm{tr}(\boldsymbol{C}) > 0$ & $\det(\boldsymbol{C}) \geq 0$.
3. $\mathrm{Tr}(\boldsymbol{C}) = \langle E_x E_x^* \rangle + \left\langle E_y E_y^* \right\rangle$ is the time averaged intensity of input light.
4. Let the polarized light (of electric field $\boldsymbol{E}_{in}$ & coherency matrix $\boldsymbol{C}_{in}$) passes through an optical element (of Jones matrix $\boldsymbol{M}$) then let output electric field be $\boldsymbol{E}_{out}$ by the equation 1.5, then output coherency matrix $\boldsymbol{C}_{out}$ is given by

$$\begin{aligned}\boldsymbol{C}_{out} = \left\langle \boldsymbol{E}_{out}\boldsymbol{E}_{out}^\dagger \right\rangle &= \left\langle (\boldsymbol{M}\boldsymbol{E}_{in})(\boldsymbol{M}\boldsymbol{E}_{in})^\dagger \right\rangle \\ &= \left\langle (\boldsymbol{M}\boldsymbol{E}_{in})\left(\boldsymbol{E}_{in}^\dagger \boldsymbol{M}^\dagger\right) \right\rangle \\ &= \boldsymbol{M}\left\langle \boldsymbol{E}_{in}\boldsymbol{E}_{in}^\dagger \right\rangle \boldsymbol{M}^\dagger \\ &= \boldsymbol{M}\,\boldsymbol{C}_{in}\,\boldsymbol{M}^\dagger \end{aligned} \tag{1.10}$$

1.3.2 Stokes parameters & Stokes vector

We see that coherency matrix $\boldsymbol{C}$ of any polarization state in table 3 can be written in the linear combination of the 4 basis given below [5]

$$\beta = \left\{ \underbrace{\begin{bmatrix}1&0\\0&1\end{bmatrix}}_{\boldsymbol{V_0}}, \underbrace{\begin{bmatrix}1&0\\0&-1\end{bmatrix}}_{\boldsymbol{V_1}}, \underbrace{\begin{bmatrix}0&1\\1&0\end{bmatrix}}_{\boldsymbol{V_2}}, \underbrace{\begin{bmatrix}0&i\\-i&0\end{bmatrix}}_{\boldsymbol{V_3}} \right\} \tag{1.11}$$

Now we can write any coherency matrix $\boldsymbol{C}$ as

$$\boldsymbol{C} = \frac{1}{2}\sum_{i=0}^{3} S_i \boldsymbol{V_i} \tag{1.12}$$

Note that all V_i's are Hermitian, so obviously is $\boldsymbol{C}$.

We call $\{S_0, S_1, S_2, S_3\}$ as a *Stokes parameter* and the values of S_i's are experimentally measurable.

A *Stokes vector* $\boldsymbol{S}$ is defined as[5]

$$\boldsymbol{S} = \begin{bmatrix} S_0 \\ S_1 \\ S_2 \\ S_3 \end{bmatrix} \tag{1.13}$$

Examples of Stokes vector for different polarization states are given below

Polarization state	$\boldsymbol{C}$	$\boldsymbol{S}$
$\lvert H\rangle$	$\begin{bmatrix} 1 & 0 \\ 0 & 0 \end{bmatrix}$	$\begin{bmatrix} 1 & 1 & 0 & 0 \end{bmatrix}^T$
$\lvert V\rangle$	$\begin{bmatrix} 0 & 0 \\ 0 & 1 \end{bmatrix}$	$\begin{bmatrix} 1 & -1 & 0 & 0 \end{bmatrix}^T$
$\lvert P\rangle$	$\frac{1}{2}\begin{bmatrix} 1 & 1 \\ 1 & 1 \end{bmatrix}$	$\begin{bmatrix} 1 & 0 & 1 & 0 \end{bmatrix}^T$
$\lvert M\rangle$	$\frac{1}{2}\begin{bmatrix} 1 & -1 \\ -1 & 1 \end{bmatrix}$	$\begin{bmatrix} 1 & 0 & -1 & 0 \end{bmatrix}^T$
$\lvert L\rangle$	$\frac{1}{2}\begin{bmatrix} 1 & -i \\ i & 1 \end{bmatrix}$	$\begin{bmatrix} 1 & 0 & 0 & 1 \end{bmatrix}^T$
$\lvert R\rangle$	$\frac{1}{2}\begin{bmatrix} 1 & i \\ -i & 1 \end{bmatrix}$	$\begin{bmatrix} 1 & 0 & 0 & -1 \end{bmatrix}^T$
Un-polarized	$\frac{1}{2}\begin{bmatrix} 1 & 0 \\ 0 & 1 \end{bmatrix}$	$\begin{bmatrix} 1 & 0 & 0 & 0 \end{bmatrix}^T$

Table 4: Stokes vector of usual polarization state

Note that all Jones vectors has Stokes vectors but converse need not to be true.

Now we see from the equation 1.12

$$\begin{bmatrix} \langle E_x E_x^* \rangle & \langle E_x E_y^* \rangle \\ \langle E_y E_x^* \rangle & \langle E_y E_y^* \rangle \end{bmatrix} = \boldsymbol{C} = \frac{1}{2}\sum_{i=0}^{3} S_i \boldsymbol{V_i} = \frac{1}{2}\begin{bmatrix} S_0 + S_1 & S_2 + iS_3 \\ S_2 - iS_3 & S_0 - S_1 \end{bmatrix} \tag{1.14}$$

From there we can write

$$\boldsymbol{S} = \begin{bmatrix} S_0 \\ S_1 \\ S_2 \\ S_3 \end{bmatrix} = \begin{bmatrix} \langle E_x E_x^* \rangle + \langle E_y E_y^* \rangle \\ \langle E_x E_x^* \rangle - \langle E_y E_y^* \rangle \\ \langle E_y E_x^* \rangle + \langle E_x E_y^* \rangle \\ i\left(\langle E_y E_x^* \rangle - \langle E_x E_y^* \rangle\right) \end{bmatrix} \tag{1.15}$$

[5]for intensity normalised Stokes vector, $\boldsymbol{s} = \begin{bmatrix} 1 & s_1 & s_2 & s_3 \end{bmatrix}$ where $s_i = S_i/S_0$

Now for a polarized light,

$$\boldsymbol{C} = \begin{bmatrix} \langle A_x^2 \rangle & \langle A_x A_y e^{-i\delta} \rangle \\ \langle A_x A_y e^{i\delta} \rangle & \langle A_y^2 \rangle \end{bmatrix} \text{ and } \boldsymbol{S} = \begin{bmatrix} S_0 \\ S_1 \\ S_2 \\ S_3 \end{bmatrix} = \begin{bmatrix} \langle A_x^2 + A_y^2 \rangle \\ \langle A_x^2 - A_y^2 \rangle \\ \langle 2A_x A_y \cos\delta \rangle \\ \langle 2A_x A_y \sin\delta \rangle \end{bmatrix} \tag{1.16}$$

where $\delta = \delta_y - \delta_x$.

1.3.3 Measurement of Stokes parameters

To measure the 4 Stokes parameter of polarized light, we have to do 4 steps experiment. In each case, we pass the light through various optical elements and measure the (time-averaged) intensity, [6]

Step I Pass the light through homogenous isotropic medium (or, free space) and measure the intensity. From table 2 and eq. 1.10, we get,

$$\begin{aligned} \boldsymbol{C}_{out} = \boldsymbol{M}\,\boldsymbol{C}_{in}\,\boldsymbol{M}^\dagger &= \begin{bmatrix} 1 & 0 \\ 0 & 1 \end{bmatrix} \frac{1}{2} \begin{bmatrix} S_0 + S_1 & S_2 + iS_3 \\ S_2 - iS_3 & S_0 - S_1 \end{bmatrix} \begin{bmatrix} 1 & 0 \\ 0 & 1 \end{bmatrix} \\ &= \frac{1}{2} \begin{bmatrix} S_0 + S_1 & 0 \\ 0 & S_0 - S_1 \end{bmatrix} \end{aligned} \tag{1.17}$$

So the measured intensity will be

$$I_0 = \mathrm{tr}(\boldsymbol{C}_{out}) = S_0 \tag{1.18}$$

Step II Pass the light through x-polarizer and measure the intensity. From table 2 and eq. 1.10, we get,

$$\boldsymbol{C}_{out} = \boldsymbol{M}\,\boldsymbol{C}_{in}\,\boldsymbol{M}^\dagger = \begin{bmatrix} 1 & 0 \\ 0 & 0 \end{bmatrix} \frac{1}{2} \begin{bmatrix} S_0 + S_1 & S_2 + iS_3 \\ S_2 - iS_3 & S_0 - S_1 \end{bmatrix} \begin{bmatrix} 1 & 0 \\ 0 & 0 \end{bmatrix} \tag{1.19}$$

So the measured intensity will be

$$I_1 = \mathrm{tr}(\boldsymbol{C}_{out}) = \frac{1}{2}(S_0 + S_1) \tag{1.20}$$

Step III Pass the light through the polarizer with transmission axis is at 45° and measure the intensity. Then from eq. 1.7, $\boldsymbol{M}$ for this polarizer will be

$$\boldsymbol{M} = R(-45^\circ) \begin{bmatrix} 1 & 0 \\ 0 & 0 \end{bmatrix} R(45^\circ) = \frac{1}{2} \begin{bmatrix} 1 & 1 \\ 1 & 1 \end{bmatrix} \tag{1.21}$$

From eq. 1.10, we get,

$$\boldsymbol{C}_{out} = \boldsymbol{M}\,\boldsymbol{C}_{in}\,\boldsymbol{M}^\dagger = \frac{1}{2} \begin{bmatrix} 1 & 1 \\ 1 & 1 \end{bmatrix} \frac{1}{2} \begin{bmatrix} S_0 + S_1 & S_2 + iS_3 \\ S_2 - iS_3 & S_0 - S_1 \end{bmatrix} \frac{1}{2} \begin{bmatrix} 1 & 1 \\ 1 & 1 \end{bmatrix} \tag{1.22}$$

So the measured intensity will be

$$I_1 = \mathrm{tr}(\boldsymbol{C}_{out}) = \frac{1}{2}(S_0 + S_2) \tag{1.23}$$

Step IV Pass the light through right circular polarizer and measure the intensity. From table 2 and eq. 1.10, we get,

$$\boldsymbol{C}_{out} = \boldsymbol{M}\,\boldsymbol{C}_{in}\,\boldsymbol{M}^{\dagger} = \frac{1}{2}\begin{bmatrix} 1 & i \\ -i & 1 \end{bmatrix} \frac{1}{2}\begin{bmatrix} S_0+S_1 & S_2+iS_3 \\ S_2-iS_3 & S_0-S_1 \end{bmatrix} \frac{1}{2}\begin{bmatrix} 1 & i \\ -i & 1 \end{bmatrix} \tag{1.24}$$

So the measured intensity will be

$$I_1 = \mathrm{tr}(\boldsymbol{C}_{out}) = \frac{1}{2}(S_0 + S_3) \tag{1.25}$$

From the equations 1.18, 1.20, 1.23 and 1.25, we can get the values of all S_i's.

Another way of measuring the Stokes parameter is passing the light beam through first wave-plate and then polarizer and measuring the intensity (see fig 1).

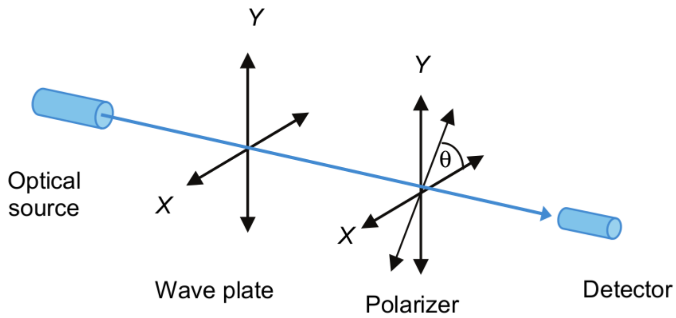

Figure 1: Experimental measurement of the Stokes polarization parameters (ref [7])

For different alignment of optical axes of wave-plate and polarizer, the intensity of the detector is,

$$I(\theta,\phi) = \frac{1}{2}[S_0 + S_1\cos 2\theta + S_2 \sin 2\theta \cos\phi - S_3 \sin 2\theta \sin\phi] \tag{1.26}$$

where ϕ is the phase shift of orthogonal electric field component introduced by wave-plate with specific orientation and θ is the transmission axis orientation angle of polarizer. [8][7]

From there one can show that,

$$S_0 = I(0,0) + I(\pi/2,0) \tag{1.27}$$
$$S_1 = I(0,0) - I(\pi/2,0) \tag{1.28}$$
$$S_1 = 2I(\pi/4,0) - S_0 \tag{1.29}$$
$$S_3 = S_0 - 2I(\pi/4,\pi/2) \tag{1.30}$$

1.3.4 Poincare sphere representation

For total intensity normalised Stokes vector is $\boldsymbol{s} = \begin{bmatrix}1 & s_1 & s_2 & s_3\end{bmatrix}^T$ where $s_i = S_i/S_0$. Observe that $\boldsymbol{s}$ is a 3-dimensional quantity. Therefore we can write,

$$\begin{bmatrix} 1 \\ s_1 \\ s_2 \\ s_3 \end{bmatrix} \rightarrow \begin{bmatrix} s_1 \\ s_2 \\ s_3 \end{bmatrix}$$

Poincare sphere representation is a coordinate system to define the state of polarization of light where the mutually orthogonal coordinate axes are $\{s_1, s_2, s_3\}$.

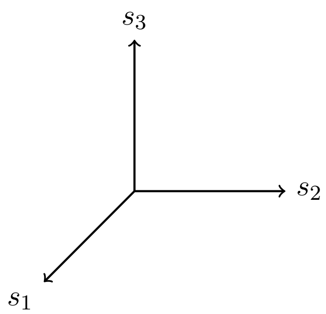

Example of special cases are

Case I For fully polarized light,

$$s_1 = \frac{A_x^2 - A_y^2}{A_x^2 + A_y^2} \tag{1.31}$$

$$s_2 = \frac{2A_y A_y \cos\delta}{A_x^2 + A_y^2} \tag{1.32}$$

$$s_3 = \frac{2A_y A_y \sin\delta}{A_x^2 + A_y^2} \tag{1.33}$$

from there we can see

$$s_1^2 + s_2^2 + s_3^2 = 1 \tag{1.34}$$

which implies that fully polarized has the locus at any point in the sphere of radius 1 in Poincare sphere representation.

Case II For fully un-polarized light,

$$s_1 = s_2 = s_3 = 0 \tag{1.35}$$

which implies that fully un-polarized has the locus at any the centre $(0, 0, 0)$ in the sphere of radius 1 in Poincare sphere representation.

Case III For partially polarized light,

$$0 < s_1^2 + s_2^2 + s_3^2 < 1 \tag{1.36}$$

1.3.5 Degree of Polarization

Degree of Polarization is the measure of polarization of light.
We define

- Total degree of polarization, $\mathcal{P} = \sqrt{s_1^2 + s_2^2 + s_3^2}$
- Degree of linear polarization $= \sqrt{s_1^2 + s_2^2}$

- Degree of circular polarization $= s_3$

Note that, $0 \leq \mathcal{P} \leq 1$

For any mixed polarization state we can decompose the Stokes vector into polarized and un-polarized components,

$$\begin{bmatrix} 1 \\ s_1 \\ s_2 \\ s_3 \end{bmatrix} = \underbrace{\begin{bmatrix} \sqrt{s_1^2 + s_2^2 + s_3^2} \\ s_1 \\ s_2 \\ s_3 \end{bmatrix}}_{\text{fully polarized, } DOP=1} + \underbrace{\begin{bmatrix} 1 - \sqrt{s_1^2 + s_2^2 + s_3^2} \\ 0 \\ 0 \\ 0 \end{bmatrix}}_{\text{un-polarized}} \tag{1.37}$$

1.3.6 Muller matrix & Evolution of Stokes vector

Similar to the Jones matrix, *Muller matrix* is a 4×4 matrix assigned for a particular optical element. Let $\mathfrak{M}$ be the Muller matrix for an optical element *s.t.*

$$\mathfrak{M} = \begin{bmatrix} \mu_{11} & \cdots & \mu_{14} \\ \vdots & \ddots & \vdots \\ \mu_{41} & \cdots & \mu_{44} \end{bmatrix}$$

then if a light of Stokes vector $\boldsymbol{S}_{in}$ passes through that optical element, then the Stokes vector of output light is given by

$$\boldsymbol{S}_{out} = \mathfrak{M}\, \boldsymbol{S}_{in} \tag{1.38}$$

Some properties of Jones matrix are

1. Resultant Muller matrix for composition of n optical elements is given by

$$\mathfrak{M} = \mathfrak{M}_1\, \mathfrak{M}_2 \ldots \mathfrak{M}_n \tag{1.39}$$

2. When th optical element is aligned at an angle θ *w.r.t.* x-axis then resultant Muller matrix (similar to Jones matrix) for this rotated optical element is given by

$$\mathfrak{M}_\theta = T^{-1}(\theta)\, \mathfrak{M}\, T(\theta) \tag{1.40}$$

where $T(\theta)$ is passive rotation matrix in Poincare sphere representation *w.r.t* s_3 axis, *s.t.*

$$T(\theta) = \begin{bmatrix} 1 & 0 & 0 & 0 \\ 0 & \cos 2\theta & \sin 2\theta & 0 \\ 0 & -\sin 2\theta & \cos 2\theta & 0 \\ 0 & 0 & 0 & 1 \end{bmatrix} \tag{1.41}$$

Note that, in eq. 1.41, if we write

$$\begin{bmatrix} 1 & 0 & 0 & 0 \\ 0 & \cos 2\theta & \sin 2\theta & 0 \\ 0 & -\sin 2\theta & \cos 2\theta & 0 \\ 0 & 0 & 0 & 1 \end{bmatrix} \longrightarrow \begin{bmatrix} \cos 2\theta & \sin 2\theta & 0 \\ -\sin 2\theta & \cos 2\theta & 0 \\ 0 & 0 & 1 \end{bmatrix} \tag{1.42}$$

we see that it is proper rotation matrix of rotation angle 2θ in Poincare sphere *w.r.t* s_3 axis. And as we know that rotation of θ of electric field results in rotation of 2θ in azimuth angle of Stokes vector in Poincare sphere.

1.3.7 Relationship between Jones & Stokes-Muller formalism

Let, $\boldsymbol{J}$ be jones vector, $\boldsymbol{M}$ be the Jones matrix, $\boldsymbol{S}$ be the Stokes vector and $\mathfrak{M}$ be the Muller matrix *s.t.* equations 1.4 and 1.38 is satisfied.

Let us define *coherency vector* of 1.9 as

$$\boldsymbol{L} = \begin{bmatrix} c_{xx} & c_{xy} & c_{yx} & c_{yy} \end{bmatrix}^T \tag{1.43}$$

and *Wolf matrix* $\boldsymbol{W}$ as

$$\boldsymbol{L}_{out} = \boldsymbol{W}\,\boldsymbol{L}_{in} \tag{1.44}$$

then the relation between Jones and Wolf matrix is

$$\boldsymbol{W} = \boldsymbol{M} \otimes \boldsymbol{M}^* \tag{1.45}$$

Now from equations 1.9 and 1.15, one can write

$$\boldsymbol{S} = \boldsymbol{A}\,\boldsymbol{L} \tag{1.46}$$

where,

$$\boldsymbol{A} = \begin{bmatrix} 1 & 0 & 0 & 1 \\ 1 & 0 & 0 & -1 \\ 0 & 1 & 1 & 0 \\ 0 & -i & i & 0 \end{bmatrix} \tag{1.47}$$

then the relation between Jones and Muller matrix is

$$\mathfrak{M} = \boldsymbol{A}\left(\boldsymbol{M} \otimes \boldsymbol{M}^*\right)\boldsymbol{A}^{-1} \tag{1.48}$$

Note that this relationship is only possible in both ways, if the light is fully polarized light as all Jones vectors has Stokes vectors but converse need not to be true.

1.4 More on Elliptically polarized light

1.4.1 Jones vector of elliptically polarized light

In this section we will discuss the generalized polarization ellipse of an EM wave. Let our electric field vector of EM wave is given by

$$\boldsymbol{E} = \begin{bmatrix} E_x \\ E_y \end{bmatrix} = \begin{bmatrix} a_1\cos(\tau + \delta_1) \\ a_2\cos(\tau + \delta_2) \end{bmatrix} \text{ where } \tau = kz - \omega t \text{ and } ta_1, a_2 \geq 0 \tag{1.49}$$

by eliminating τ we get,

$$\frac{1}{a_1^2}E_x^2 + \frac{1}{a_2^2}E_y^2 - \frac{2\cos\delta}{a_1 a_2}E_x E_y = \sin^2(\delta) \tag{1.50}$$

where $\delta = \delta_2 - \delta_1$. The eq. 1.50 is equation of circle when $a_1 = a_2$, otherwise, of ellipse. [2]

Now we do the change of basis $\{E_x, E_y\} \longmapsto \{E_\xi, E_\eta\}$ (See fig. 2) *s.t.* electric field in $\{E_\xi, E_\eta\}$ basis be

$$\boldsymbol{E} \rightarrow \boldsymbol{F}$$
$$\boldsymbol{F} = \begin{bmatrix} E_\xi \\ E_\eta \end{bmatrix} = \begin{bmatrix} a\cos(\tau+\delta_0) \\ \pm b\sin(\tau+\delta_0) \end{bmatrix} \text{ where } a \geq b \geq 0 \tag{1.51}$$

which is parametric form of canonical ellipse[6] in $\{E_\xi, E_\eta\}$ basis.

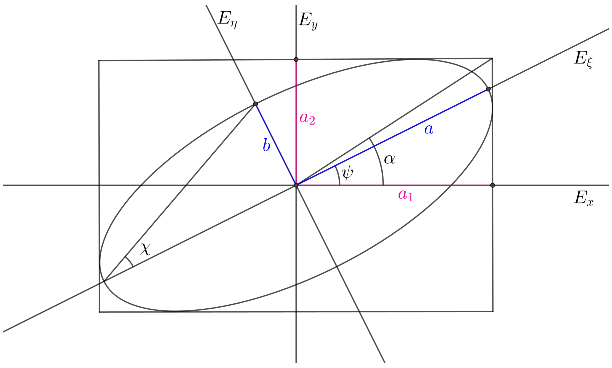

Figure 2: Polarization ellipse

Let ψ be the azimuth angle of the ellipse then

$$\boldsymbol{F} = R(\psi)\,\boldsymbol{E} \tag{1.52}$$
$$\Rightarrow \begin{bmatrix} E_\xi \\ E_\eta \end{bmatrix} = \begin{bmatrix} \cos\psi & \sin\psi \\ -\sin\psi & \cos\psi \end{bmatrix} \begin{bmatrix} E_x \\ F_y \end{bmatrix} \tag{1.53}$$
$$\Rightarrow \begin{bmatrix} a\cos(\tau+\delta_0) \\ \pm b\sin(\tau+\delta_0) \end{bmatrix} = \begin{bmatrix} \cos\psi & \sin\psi \\ -\sin\psi & \cos\psi \end{bmatrix} \begin{bmatrix} a_1\cos(\tau+\delta_1) \\ a_2\cos(\tau+\delta_2) \end{bmatrix} \tag{1.54}$$

We want value of a, b, After some tedious calculation [2], we reach to some important results, given below

$$a^2 + b^2 = a_1^2 + a_2^2 \tag{1.55}$$
$$\pm\, ab = a_1 a_2 \sin\delta \tag{1.56}$$
$$\tan\chi := \pm\frac{b}{a} \text{ where } \chi \in [-\frac{\pi}{4}, \frac{\pi}{4}] \tag{1.57}$$
$$\tan\alpha := \frac{a_2}{a_1} \text{ where } \alpha \in [0, \frac{\pi}{2}] \tag{1.58}$$
$$\tan 2\psi = \tan 2\alpha \cos\delta \tag{1.59}$$
$$\sin 2\chi = \sin 2\alpha \sin\delta \tag{1.60}$$

where ψ is the *azimuth* and χ is *ellipticity* of the polarization ellipse.

To see the handedness of the rotation of electric field vector in transverse plane,

Case I For right-handed polarization, $\sin\delta > 0$, then from equations 1.56, and 1.57, we can say

$$\tan\chi \geq 0 \Rightarrow \chi \in \left(0, \frac{\pi}{4}\right]$$

[6] $\pm$ before b denotes the handedness of the rotation of electric field vector in transverse plane.

Case II Similarly for left-handed polarization, $\sin\delta < 0$, then from equations 1.56, and 1.57, we can say

$$\tan\chi \leq 0 \Rightarrow \chi \in \left[-\frac{\pi}{4}, 0\right)$$

Now the Jones vector of elliptical polarization in the form of ellipticity and azimuth will be, [1]

$$\boldsymbol{J} = \begin{bmatrix} \cos\psi\cos\chi - i\sin\psi\sin\chi \\ \sin\psi\cos\chi + i\cos\psi\sin\chi \end{bmatrix} \tag{1.61}$$

1.4.2 Stokes vector and corresponding Poincare representation

From the eq. 1.16, we can write for our case,

$$\boldsymbol{S} = \begin{bmatrix} S_0 \\ S_1 \\ S_2 \\ S_3 \end{bmatrix} = \begin{bmatrix} a_1^2 + a_2^2 \\ a_1^2 - a_2^2 \\ 2a_1a_2\cos\delta \\ 2a_1a_2\sin\delta \end{bmatrix} = S_0 \begin{bmatrix} 1 \\ \cos 2\chi\cos 2\psi \\ \cos 2\chi\sin 2\psi \\ \sin 2\chi \end{bmatrix} \tag{1.62}$$

So in Poincare sphere representation with axes $\{S_1, S_2, S_3\}$, the required vector is

$$S_0 \begin{bmatrix} 1 \\ \cos 2\chi\cos 2\psi \\ \cos 2\chi\sin 2\psi \\ \sin 2\chi \end{bmatrix} \longrightarrow (S_0\cos 2\chi\cos 2\psi, S_0\cos 2\chi\sin 2\psi, S_0\sin 2\chi) \tag{1.63}$$

The evolution of azimuth (ψ) and ellipticity (χ) of the polarization state in Poincare representation is shown in the figure 3.

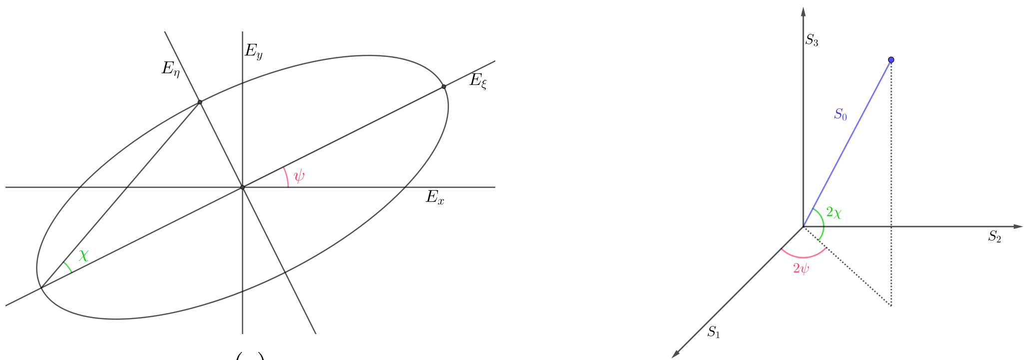

(a) (b)

Figure 3: polarization ellipse and corresponding Poincare representation

For any ψ and χ in the domain, the locus of state of polarization in Poincare sphere representation will always be on the sphere about origin of radius S_0. The pole and equatorial positions denotes the circular and linear polarization, respectively.

2 GAUSSIAN BEAM

2.1 Introduction

In optics and laser physics, the Gaussian beam stands as a fundamental concept, where the intensity of the light beam follows Gaussian curve. Its elegance lies in the fact that, it propagate over long distances with minimal divergence and diffraction. This distinctive feature makes it a preferred choice in a wide array of applications in optics and laser physics. Here we will briefly discuss about the different modes of Gaussian beams, as well as their properties.

2.2 Paraxial wave equation

From Maxwell's 3-D wave equation for electric field in vacuum,

$$\nabla^2 \boldsymbol{E}(\boldsymbol{r},t) - \frac{1}{c^2}\frac{\partial^2}{\partial t^2}\boldsymbol{E}(\boldsymbol{r},t) = 0 \tag{2.1}$$

Here we will consider the scalar form of the equation.

To find the scalar solution, let our first ansatz be,

$$E(x,y,z,t) = F(x,y,z)e^{i\omega t} \tag{2.2}$$

Putting it in eq. 2.1, we get time -independent *Helmholtz equation i.e.*

$$\nabla^2 F(x,y,z) + k^2 F(x,y,z) = 0 \text{ where } k^2 = \frac{\omega^2}{c^2} \tag{2.3}$$

For light to travel in z-direction, our 2nd ansatz be,

$$F(\boldsymbol{r}) = \psi(x,y,z)e^{-ikz} \tag{2.4}$$

Considering the slowly varying envelope approximation[1] that,

$$\left|\frac{\partial^2\psi}{\partial z^2}\right| \ll k\left|\frac{\partial\psi}{\partial z}\right| \ll k^2\left|\psi\right| \tag{2.5}$$

and putting 2.4 in eq. 2.3 gives *Paraxial wave equation*,

$$\nabla_T^2\psi - 2ik\frac{\partial\psi}{\partial r} = 0 \tag{2.6}$$

where transverse Laplacian, $\nabla_T = \frac{\partial^2}{\partial x^2}+\frac{\partial^2}{\partial y^2}$ or in cylindrical coordinate, $\nabla_T = \frac{1}{r}\frac{\partial}{\partial r}\left(r\frac{\partial}{\partial r}\right)+\frac{1}{r^2}\frac{\partial^2}{\partial\phi^2}$.

2.3 Scalar wave solution - Gaussian beam

We will solve the paraxial wave equation in cylindrical coordinate $\{r,\phi,z\}$. To get a solution for which intensity is of Gaussian like and radially symmetric (*i.e.* no variation with ϕ), our first ansatz be, [11][10]

$$\psi(\boldsymbol{r},z) = A\exp\left[-i\left(p(z)+\frac{kr^2}{2q(z)}\right)\right] = A\underbrace{\exp\left[-ip(z)\right]}_{\text{first term}}\underbrace{\exp\left[-i\frac{kr^2}{2q(z)}\right]}_{\text{second term}} \tag{2.7}$$

where second term is related to Gaussian intensity and first term is additional phase factor. Putting this, in eq, 2.6, we get

$$\left[\frac{k^2}{q^2}\left(\frac{dq}{dz}-1\right)r^2-2k\left(\frac{dp}{dz}+\frac{i}{q}\right)\right]\psi=0 \tag{2.8}$$

To satisfy this, for all r, we get

$$\frac{dq}{dz}-1=0 \tag{2.9}$$

$$\frac{dp}{dz}+\frac{i}{q}=0 \tag{2.10}$$

Let's first calculate eq. 2.9.

$$\frac{dq}{dz}-1=0 \Rightarrow q(z)=z+q_0 \tag{2.11}$$

putting this in the second term of expression 2.7 at $z=0$,

$$\exp\left[-i\frac{kr^2}{2q(0)}\right]=\exp\left[-i\frac{kr^2}{2q_0}\right] \tag{2.12}$$

which is a phase factor does not give Gaussian intensity. So to get Gaussian intensity, q_0 must be imaginary. Let $q_0=iz_0$, then

$$\boxed{q(z)=z+iz_0} \tag{2.13}$$

Now the second term of expression 2.7 at $z=0$ be,

$$\exp\left[-\frac{kr^2}{2z_0}\right]=\exp\left[-\frac{r^2}{w_0^2}\right] \tag{2.14}$$

where

$$w_0^2=\frac{2z_0}{k}=\frac{\lambda z_0}{\pi} \Rightarrow \boxed{z_0=\frac{\pi w_0^2}{\lambda}} \tag{2.15}$$

We call z_0 *confocal parameter* or *Rayleigh range* of the beam.

Now from expression 2.13, we calculate $1/q(z)$.

$$\frac{1}{q(z)}=\frac{1}{z+iz_0}=\frac{z}{z^2+z_0^2}-i\,\frac{z_0}{z^2+z_0^2} \tag{2.16}$$

Then the second term of expression 2.7 be,

$$\exp\left[-i\frac{kr^2}{2q(z)}\right]=\underbrace{\exp\left[-\frac{kr^2z_0}{2(z^2+z_0^2)}\right]}_{\text{term A}}\underbrace{\exp\left[-i\frac{kr^2z}{2(z^2+z_0^2)}\right]}_{\text{term B}} \tag{2.17}$$

Write term A of 2.17 as

$$\exp\left[-\frac{kr^2z_0}{2(z^2+z_0^2)}\right]=\exp\left[-\frac{r^2}{w^2(z)}\right] \tag{2.18}$$

which is Gaussian, where

$$\boxed{w^2(z) = w_0^2\left[1 + \left(\frac{z}{z_0}\right)^2\right]} \tag{2.19}$$

We call $w(z)$ *physical radius/half-width* of the beam.

Write term B of 2.17 as

$$\exp\left[-i\frac{kr^2 z}{2(z^2 + z_0^2)}\right] = \exp\left[-i\frac{kr^2}{2R(z)}\right] \tag{2.20}$$

where

$$\boxed{R(z) = z\left[1 + \left(\frac{z_0}{z}\right)^2\right]} \tag{2.21}$$

We know for spherical wave,

$$E(\boldsymbol{r}, t) \sim \frac{1}{r}e^{i(\omega t - kr)} \tag{2.22}$$

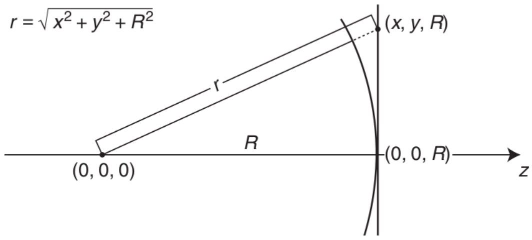

Figure 4: Radius of curvature of spherical wavefront (Ref. [9])

Let R be the radius of curvature of spherical wavefront. Now for any point $\boldsymbol{r} = (x, y, R)$ on $z = R$ plane, r will be

$$r = \sqrt{x^2 + y^2 + R^2} \tag{2.23}$$

For collimated beam, we restrict radius of curvature measurement near $\boldsymbol{r} = (0, 0, R)$, so

$$r = \sqrt{x^2 + y^2 + R^2} \approx R + \frac{x^2 + y^2}{2R} \tag{2.24}$$

Now from 2.22,

$$E(\boldsymbol{r}, t) \sim \frac{1}{r}e^{i\omega t}e^{-ikr}e^{-ik\frac{x^2+y^2}{2R}} \tag{2.25}$$

comparing with 2.2,

$$\psi(x, y, z) \sim e^{-ik\frac{x^2+y^2}{2R}} \tag{2.26}$$

comparing 2.26 in the above expression with term B of 2.17, we conclude that $R(z)$ in 2.21 is *radius of curvature* of wavefront near $r = 0$ of collimated beam in far field.

Putting 2.19 and 2.21 in eq. 2.16,

$$\boxed{\frac{1}{q(z)} = \frac{1}{R(z)} - i\,\frac{\lambda}{\pi w^2(z)}} \tag{2.27}$$

Now we simplify the first term in 2.7. Putting 2.13 in 2.10 and by solving the differential equation, we get,

$$\frac{dp}{dz} = \frac{-i}{q} = \frac{-i}{z + iz_0} \Rightarrow i\,p(z) = \ln\left[1 - i\frac{z}{z_0}\right] \tag{2.28}$$

As we can write

$$1 - i\frac{z}{z_0} = \sqrt{1 + \left(\frac{z}{z_0}\right)^2}\,\exp\left[-i\,\tan^{-1}\left(\frac{z}{z_0}\right)\right]$$

putting this in the above expression of $i\,p(z)$, our final expression will be

$$i\,p(z) = \frac{1}{2}\ln\left[1 + \left(\frac{z}{z_0}\right)^2\right] - i\,\tan^{-1}\left(\frac{z}{z_0}\right) \tag{2.29}$$

Finally putting 2.27 and 2.29 in 2.7, we get, [11][10]

$$\begin{aligned}
\psi(\boldsymbol{r}, z) &= A\exp\left[-i\left(p(z) + \frac{kr^2}{2q(z)}\right)\right] \\
&= A\exp\left[-\frac{1}{2}\ln\left[1 + \left(\frac{z}{z_0}\right)^2\right] + i\,\tan^{-1}\left(\frac{z}{z_0}\right) - i\frac{kr^2}{2}\left(\frac{1}{R(z)} - i\,\frac{\lambda}{\pi w^2(z)}\right)\right] \\
&= \frac{A}{\sqrt{1 + \left(\frac{z}{z_0}\right)^2}}\exp\left(i\,\tan^{-1}\left(\frac{z}{z_0}\right)\right)\exp\left(-i\frac{kr^2}{2R(z)}\right)\exp\left(-\frac{r^2}{w^2(z)}\right) \\
\Rightarrow \psi(\boldsymbol{r}, z) &= A\,\underbrace{\left(\frac{w_0}{w(z)}\right)}_{\text{term I}}\,\underbrace{\exp\left(i\,\tan^{-1}\left(\frac{z}{z_0}\right)\right)}_{\text{term II}}\,\underbrace{\exp\left(-i\frac{kr^2}{2R(z)}\right)}_{\text{term III}}\,\underbrace{\exp\left(-\frac{r^2}{w^2(z)}\right)}_{\text{term IV}}
\end{aligned} \tag{2.30}$$

In that expression,

1. Term I $\longrightarrow$ related to spreading of beam along propagation in z.
2. Term II $\longrightarrow$ related to *Gouy phase*.
3. Term III $\longrightarrow$ gives radius of curvature of beam wave front.
4. Term IV $\longrightarrow$ gives radially symmetric Gaussian intensity profile.

2.4 Characteristics of Gaussian Beam

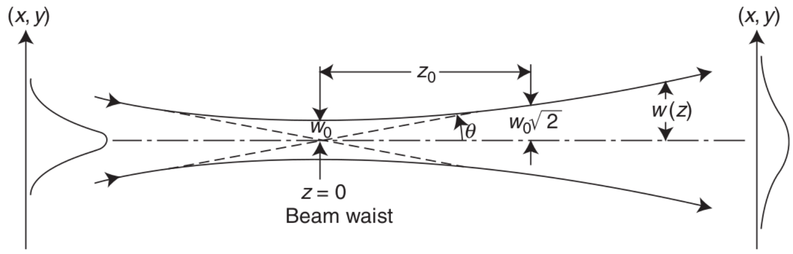

Figure 5: A beam profile (Ref. [9])

Some characteristics of Gaussian beam are

1. *Intensity* of Gaussian beam in any transverse plain is,

$$
\begin{aligned}
I(r,z) &= \frac{1}{2}\epsilon_0 c|E^*E| = \frac{1}{2}\epsilon_0 c|\psi^*\psi| \\
&= \frac{1}{2}\epsilon_0 c|A|^2\left(\frac{w_0}{w(z)}\right)^2 \exp\left(-\frac{2r^2}{w^2(z)}\right)
\end{aligned} \tag{2.31}
$$

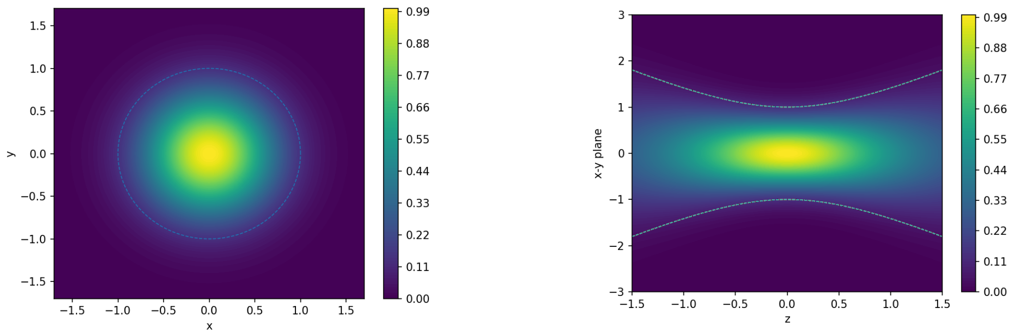

(a) Intensity variation in a cross section

(b) Intensity variation along z-axis

Figure 6: Gaussian intensity profile for $z_0 = 1, w_0 = 1$

2. *Rate of energy* of Gaussian beam passes through any transverse plain is given by

$$
\begin{aligned}
W &= \iint_{-\infty}^{\infty} dx\, dy\, I(x,y,z) \\
&= \frac{1}{2}\epsilon_0 c|A|^2\left(\frac{w_0}{w(z)}\right)^2 \iint_{-\infty}^{\infty} dx\, dy\, \exp\left(-\frac{2(x^2+y^2)}{w^2(z)}\right) \\
&= \frac{1}{2}\epsilon_0 c|A|^2\left(\frac{w_0}{w(z)}\right)^2 \int_{-\infty}^{\infty} dx\, \exp\left(-\frac{2x^2}{w^2(z)}\right) \int_{-\infty}^{\infty} dy\, \exp\left(-\frac{2y^2}{w^2(z)}\right) \\
&= \frac{1}{2}\epsilon_0 c|A|^2\left(\frac{w_0}{w(z)}\right)^2 (\sqrt{\pi}w(z))^2 = \frac{1}{2}\epsilon_0 c|A|^2 w_0^2
\end{aligned} \tag{2.32}
$$

which is constant throughout the propagation along z-axis.

3. *Radius of curvature* $R(z)$ of the wavefront is given by

$$R(z) = z\left[1 + \left(\frac{z_0}{z}\right)^2\right] \tag{2.33}$$

For $z = 0$ $R \to \infty$

For $z >> z_0$, then $R \approx z$

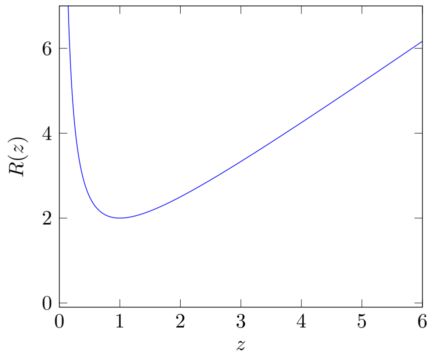

Figure 7: Variation of radius of curvature with z ($z_0 = 1$)

4. *Beam half-width* (see fig. 5) is given by

$$w(z) = w_0\sqrt{1 + \left(\frac{z}{z_0}\right)^2} \tag{2.34}$$

For $z = 0$, then $w = w_0$ (*Beam waist*)

For $z >> z_0$, then $w(z) = w_0\frac{z}{z_0}$

Diffraction angle at far field is given by

$$2\theta = 2\lim_{z\to\infty}\frac{dw}{dz} = 2\frac{w_0}{z_0} = \frac{2\lambda}{\pi w_0} \tag{2.35}$$

Effective area of the beam in a cross section is $\frac{1}{2}\pi w^2(z)$

5. *Gouy phase* represents the difference in phase shift of a Gaussian beam *w.r.t.* a plane wave of the same wavelength near $r = 0$. [15] Gouy phase of a Gaussian beam is given by

$$\phi_g(z) = \tan^{-1}\left(\frac{z}{z_0}\right) \tag{2.36}$$

The Gouy phase vary form $-\pi/2$ to $\pi/2$ continuously as z goes from $-\infty$ to ∞, shown in fig. 8

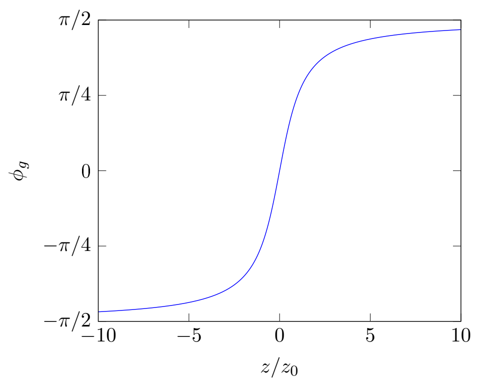

Figure 8: Variation of Gouy phase with z

6. Inside Rayleigh length (z_0), the laser beam is highly collimated and intensity is also very high. So gain medium is kept in between $z = -z_0$ and z_0 to get maximum stimulated emission from gain medium.

2.5 Beam Tracing using ABCD matrix

Like ray tracing using ABCD matrix, beam tracing is also done using ABCD matrix. We know that q parameter gives all the characteristic of the beam as

$$q(z) = z + iz_0$$
$$\frac{1}{q(z)} = \frac{1}{R(z)} - i\frac{\lambda}{\pi w^2(z)}$$

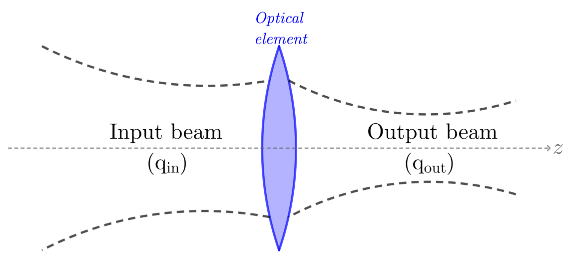

Figure 9: Schematic of beam tracing

By using ABCD matrix we can understand the change in q parameter of input and output the Gaussian beam, say q_{in} and q_{out} respectively. Let the ABCD matrix of the optical element is

$$\begin{bmatrix} A & B \\ C & D \end{bmatrix} \tag{2.37}$$

Then relation between q_{in} and q_{out} is

$$q_{out} = \frac{A\,q_{in} + B}{C\,q_{in} + D} \tag{2.38}$$

2.6 Resonator stability and resonator mode-frequency

Now we will discuss about the *resonator stability* for the Gaussian beam. The resonator cavity (or optical cavity) is made of two highly reflecting mirror align in particular manner so that light confined in the cavity reflects multiple times, producing modes with certain resonance frequencies. [12] If a Gaussian beam is to be a mode of a resonator with spherical mirrors, then radius of curvature of beam wave-front must be equal to that of the mirror.

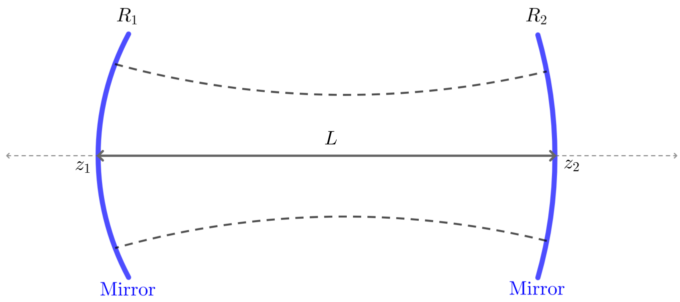

Figure 10: Schematic of beam resonator of two mirrors of radius of curvature R_1 & R_2

Let radius of curvature of first and second mirror are R_1 and R_2 respectively, length of resonator cavity is L, then [9]

$$R(z_1) = z_1 + \frac{z_0^2}{z_1} = -R_1 \tag{2.39}$$

$$R(z_2) = z_2 + \frac{z_0^2}{z_2} = R_2 \tag{2.40}$$

$$z_2 - z_1 = L \tag{2.41}$$

Lets define,

$$g_i = 1 - \frac{L}{R_i} \tag{2.42}$$

where $R_i > 0$ for concave and < 0 for convex mirror. By considering the four relation, and the properties of Gaussian beam, we get, [9]

1. Mirror locations *w.r.t.* beam waist location, z_0 be

$$z_1 = -\frac{Lg_2(1-g_1)}{g_1 + g_2 - 2g_1g_2} \tag{2.43}$$

$$z_2 = z_1 + L \tag{2.44}$$

2. Let spot sizes of beam at first, second mirrors and beam waist be w_1, w_2 and w_0 respectively, then

$$w_1 = \left(\frac{\lambda L}{\pi}\right)^{1/2} \left(\frac{g_2}{g_1(1-g_1g_2)}\right)^{1/4} \tag{2.45}$$

$$w_2 = \left(\frac{\lambda L}{\pi}\right)^{1/2} \left(\frac{g_1}{g_2(1-g_1g_2)}\right)^{1/4} \tag{2.46}$$

$$w_0 = \left(\frac{\lambda L}{\pi}\right)^{1/2} \left(\frac{g_1g_2(1-g_1g_2)}{(g_1+g_2-2g_1g_2)^2}\right)^{1/4} \tag{2.47}$$

Note that w_0 to be a real value,

$$\begin{aligned} &g_1 g_2(1 - g_1 g_2) > 0 \\ \Rightarrow &\boxed{g_1 g_2 \notin [0,1]} \end{aligned} \tag{2.48}$$

This is the *condition of stable resonator.* The cases when $g_1 g_2 = 0, 1$ is neither stable nor unstable, is called *marginal stability*.

From 2.4 and 2.30, we see that the spatial phase of Gaussian beam near the centroid (*i.e.* $r \approx 0$) be

$$\Phi(z) = kz - \tan^{-1}\left(\frac{z}{z_0}\right) \tag{2.49}$$

For light confined in the cavity to be in standing wave mode, phase change in a round trip *i.e.* from first mirror after reflecting at second mirror to again first mirror, should be an integral multiple of 2π. So phase change from first mirror to second mirror is an integral multiple of π. Then

$$\begin{aligned} \Phi(z_2) - \Phi(z_1) &= m\pi \\ k(z_2 - z_1) - \left[\tan^{-1}\left(\frac{z_2}{z_0}\right) - \tan^{-1}\left(\frac{z_1}{z_0}\right)\right] &= m\pi, \text{ where } m = 0, \pm 1, \pm 2, \ldots \end{aligned} \tag{2.50}$$

If the mode frequency is ν, $k = 2\pi\nu/c$, then

$$\nu_m = \frac{c}{2L}\left[m + \frac{1}{\pi}\cos^{-1}(\sqrt{g_1 g_2})\right] \tag{2.51}$$

This is *longitudinal mode* of Gaussian beam.

2.7 Different modes of Gaussian beams

Here we will discuss mainly two types of higher order Gaussian beams *i.e.*

1. Hermite-Gaussian (HG) beam
2. Laguerre-Gaussian (LG) beam

2.7.1 Hermite-Gaussian beam

In the expression 2.30, we get the radially symmetric Gaussian beam solution. But we now seek higher order solution of Gaussian beam which is rectangular symmetric.

Lets take the ansatz as,

$$\psi(\boldsymbol{r}, z) = A\, g\left(\frac{x}{w(z)}\right) h\left(\frac{y}{w(z)}\right) \exp\left[-i\left(p(z) + \frac{kr^2}{2q(z)}\right)\right] \tag{2.52}$$

Putting this in Paraxial wave equation 2.6, and solving the differential equation, [9] we get,

$$\begin{aligned} \psi_{m,n}(\boldsymbol{r}, z) =& A\left(\frac{w_0}{w(z)}\right) H_m\left(\frac{\sqrt{2}x}{w(z)}\right) H_n\left(\frac{\sqrt{2}y}{w(z)}\right) \exp\left(-\frac{r^2}{w^2(z)}\right) \cdot \\ & \exp\left(i\,(m + n + 1)\tan^{-1}\left(\frac{z}{z_0}\right) - i\frac{kr^2}{2R(z)}\right) \end{aligned} \tag{2.53}$$

where H_i is *i th degree Hermite polynomial* and other symbols are as usual. See for $m = 0 = n$ we recover the Gaussian solution of 2.30 which we call as *zero order* HG beam. For different values of m an n, we will get diferent type of higher order HG beam, these are called *transverse electromagnetic mode* of order (m, n) or, TEM_{mn}.

Some characteristics of HG beams are given below,

1. *Intensity* of HG beam is given by

$$I_{m,n}(x,y,z) = \frac{c\epsilon}{2}|A|^2 \left[H_m\left(\frac{\sqrt{2}x}{w(z)}\right)\right]^2 \left[H_n\left(\frac{\sqrt{2}y}{w(z)}\right)\right]^2 \exp\left(\frac{2(x^2+y^2)}{w^2(z)}\right) \quad (2.54)$$

Due to the number of zeros equals the degree of Hermite polynomial, we will see m number of horizontal and n number of vertical node in intensity profile of the TEM_{mn} beam. See figure 12.

2. *Rate of energy* of HG beam passes through any transverse plain is given by

$$\begin{aligned} W &= \iint_{-\infty}^{\infty} dx\, dy\, I(x,y,z) \\ &= \frac{1}{2}\epsilon_0 c|A|^2 \left(\frac{w_0}{w(z)}\right)^2 \int_{-\infty}^{\infty} dx\, \exp\left(-\frac{2x^2}{w^2(z)}\right) \left[H_m\left(\frac{\sqrt{2}x}{w(z)}\right)\right]^2 \end{aligned} \quad (2.55)$$

the integration terms of 2.55 are in the form of

$$\int_{-\infty}^{\infty} H_l \exp(-a\xi^2)d\xi = \int_{-\infty}^{\infty} \left(\sum_{k=0}^{l} c_k \xi_k\right) \exp(-a\xi^2)d\xi = \sum_{k=0}^{l} c_k \int_{-\infty}^{\infty} \xi_k \exp(-a\xi^2)d\xi$$

as the values of $\int_{-\infty}^{\infty} \xi_k \exp(-a\xi^2)d\xi$ is fixed[7] and for finite value of l, W is finite and constant throughout the propagation along z-axis.

3. *Radius of curvature* of HG beam is same as simple Gaussian beam for all modes.

4. *Gouy phase* for different order HG beam is given by

$$\phi_g(\eta, z) = \eta \tan^{-1}\left(\frac{z}{z_0}\right) \text{ where } \eta = m + n + 1 \quad (2.56)$$

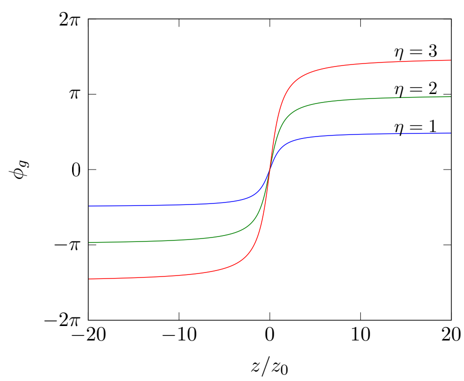

Figure 11: Variation of Gouy phase with z for HG beam

[7] as n^{th} moment of a random variable of Gaussian distribution has a fixed value for a particular integer values of n [17]

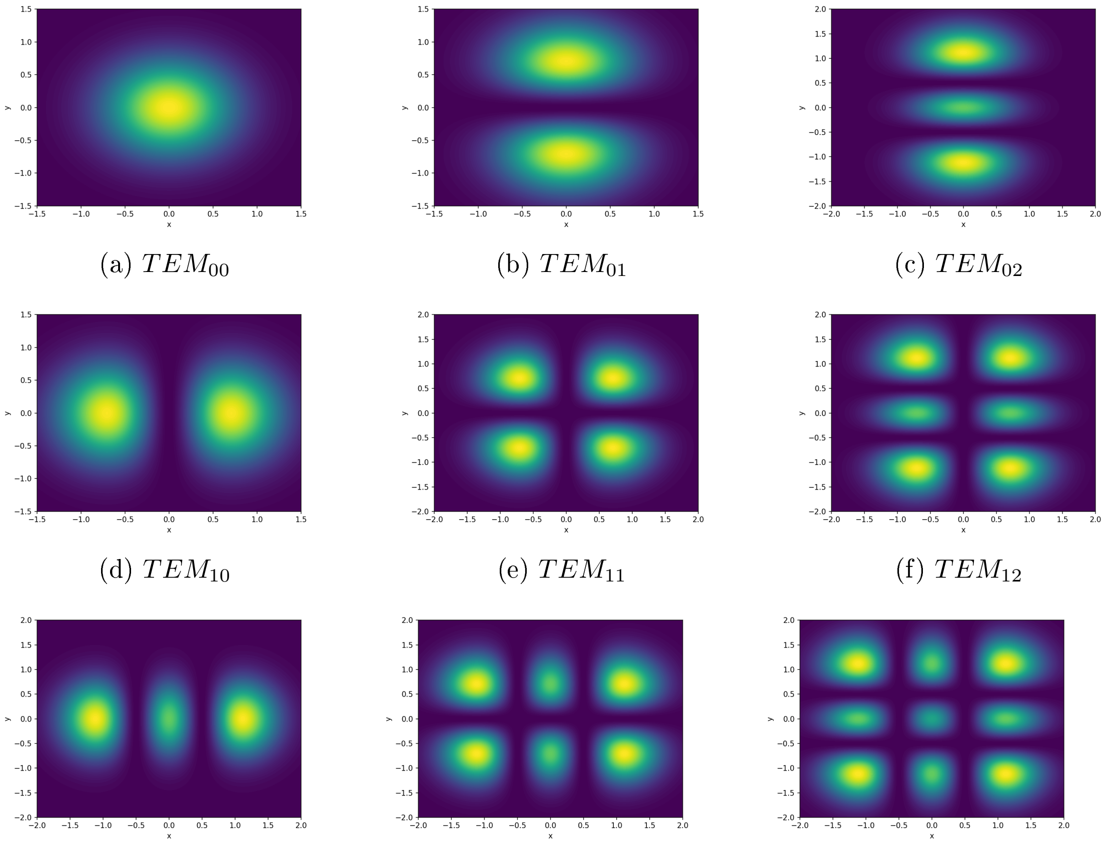

(a) TEM_{00} (b) TEM_{01} (c) TEM_{02}

(d) TEM_{10} (e) TEM_{11} (f) TEM_{12}

(g) TEM_{20} (h) TEM_{21} (i) TEM_{22}

Figure 12: Intensity variation for different TEM in a cross section ($z = 0, z_0 = 1, w_0 = 1$)

2.7.2 Laguerre-Gaussian beam

In the expression 2.30, we get the radially symmetric Gaussian beam solution. But we now seek higher order solution of Gaussian beam which is not radially symmetric i.e. vary with ϕ.

Let's take the ansatz as,

$$\psi(r,\phi,z) = A\, g\left(\frac{y}{w(z)}\right) \exp\left[-i\left(p(z) + \frac{kr^2}{2q(z)} + l\phi\right)\right] \tag{2.57}$$

Putting this in Paraxial wave equation 2.6, and solving the differential equation, [18][11] we get

$$\begin{aligned}\psi_{p,l}(r,\phi,z) =& A\,\frac{w_0}{w(z)}\left[\frac{r\sqrt{2}}{w(z)}\right]^{|l|} L_p^{|l|}\left(\frac{2r^2}{w^2(z)}\right)\exp\left(-\frac{r^2}{w^2(z)}\right)\cdot \\ & \exp\left(-il\phi + i(2p+l+1)\tan^{-1}\left(\frac{z}{z_0}\right) - i\frac{kr^2}{2R(z)}\right)\end{aligned} \tag{2.58}$$

where l is *vortex quantum number*, takes integer value, $L_p^{|l|}$ is *associated Laguerre polynomial* and other terms are as usual.

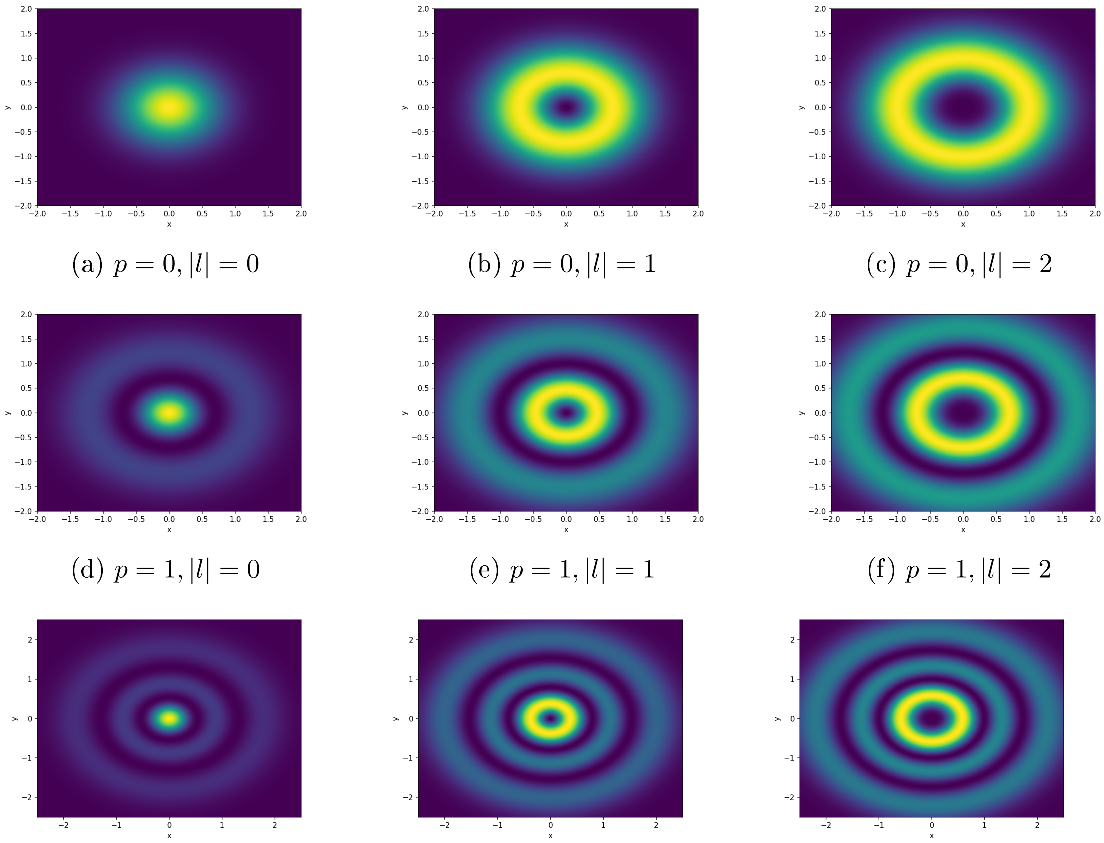

(a) $p = 0, |l| = 0$ (b) $p = 0, |l| = 1$ (c) $p = 0, |l| = 2$

(d) $p = 1, |l| = 0$ (e) $p = 1, |l| = 1$ (f) $p = 1, |l| = 2$

(g) $p = 2, |l| = 0$ (h) $p = 2, |l| = 1$ (i) $p = 2, |l| = 2$

Figure 13: Intensity variation for different modes in a cross section ($z = 0, z_0 = 1, w_0 = 1$)

Some characteristics of HG beams are given below,

1. *Intensity* of LG beam is given by

$$I_{p,l}(r,z) = \frac{c\epsilon}{2}|A|^2 \left[\frac{w_0}{w(z)}\right]^2 \left[\frac{r\sqrt{2}}{w(z)}\right]^{2|l|} \left[L_p^{|l|}\left(\frac{2r^2}{w^2(z)}\right)\right]^2 \exp\left(-\frac{2r^2}{w^2(z)}\right) \tag{2.59}$$

   See intensity plot for corresponding LG beam in figure 13. For $|l| \neq 0$ the intensity of centre is zero and the value of p denotes the number of radial nodes as $L_p^{|l|}$ has p number of zeros.

2. *Rate of energy* of HG beam passes through any transverse plain is given by

$$\begin{aligned} W &= \iint_{-\infty}^{\infty} dx\, dy\, I(x,y,z) \\ &= \frac{1}{2}\epsilon_0 c|A|^2 \left(\frac{w_0}{w(z)}\right)^2 \int_{-\infty}^{\infty} dx \left(\frac{2r^2}{w^2(z)}\right)^{|l|} \left[L_p^{|l|}\left(\frac{2r^2}{w^2(z)}\right)\right]^2 \exp\left(-\frac{2r^2}{w^2(z)}\right) \end{aligned} \tag{2.60}$$

   By same argument as HG beam, we can conclude W is finite and constant throughout the propagation along z-axis

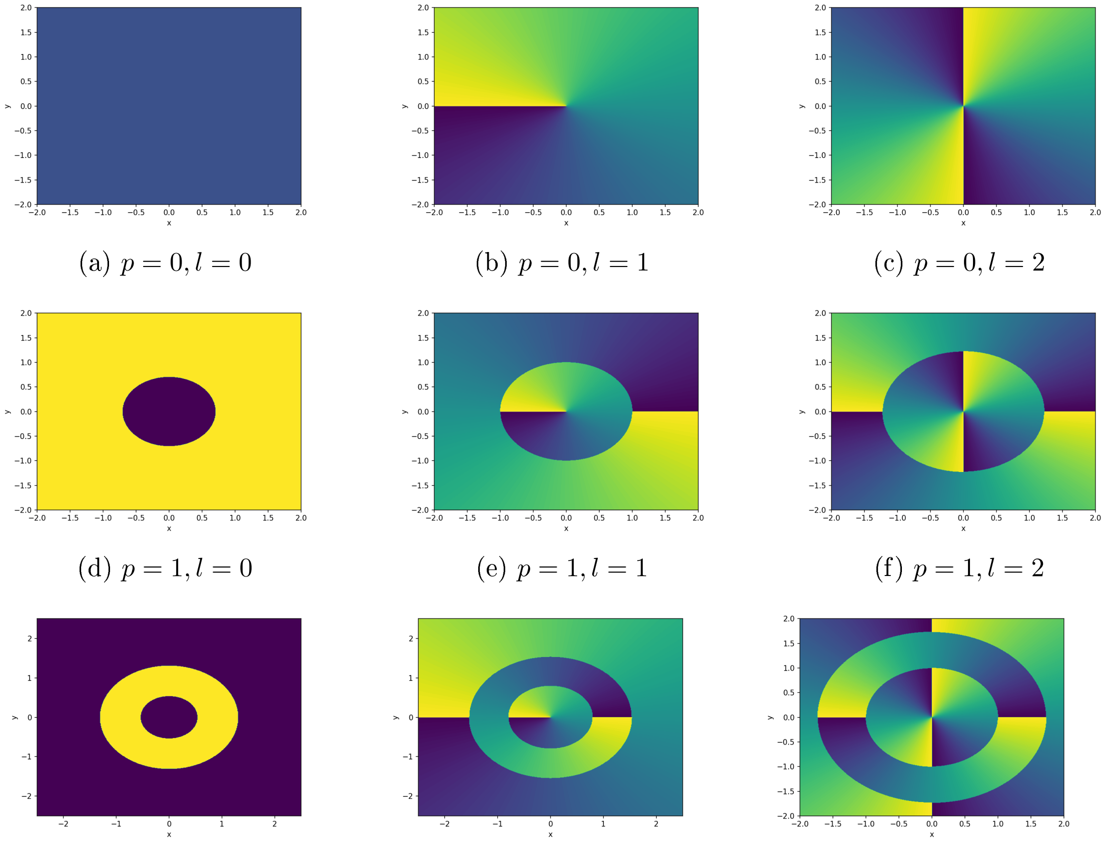

(a) $p = 0, l = 0$ (b) $p = 0, l = 1$ (c) $p = 0, l = 2$

(d) $p = 1, l = 0$ (e) $p = 1, l = 1$ (f) $p = 1, l = 2$

(g) $p = 2, l = 0$ (h) $p = 2, l = 1$ (i) $p = 2, l = 2$

Figure 14: Phase variation for different modes in a cross section ($z = 0, z_0 = 1, w_0 = 1$)

3. *Phase* of the LG beam, unlike Gaussian beam, not only depends on the r and z, but also on ϕ. Phase of LG beam is given by

$$\Phi_{LG}(r, \phi, z) = \arg(\psi_{p,l}(r, \phi, z)) \tag{2.61}$$

   Phase plot for different order of LG beam at $z = 0$ is given in figure 14.

4. As we will see later section, unlike the HG beam, LG bream carry orbital angular momentum due to its phase variation *w.r.t.* ϕ which results helical phase-front of the beam.

2.8 Maxwell-Gaussian beam (with polarization)

According to [13], let us consider electric field $\boldsymbol{E}$ and magnetic field $\boldsymbol{E}$ of a EM wave propagating in z-direction, we write, in Cartesian coordinate,[8]

$$\boldsymbol{E}(\boldsymbol{r},t) = \boldsymbol{E_0}\, e^{i(kz-\omega t)} = \begin{bmatrix} E_{0x}(\boldsymbol{r}) \\ E_{0y}(\boldsymbol{r}) \\ E_{0y}(\boldsymbol{r}) \end{bmatrix} e^{i(kz-\omega t)} \tag{2.62}$$

$$\boldsymbol{B}(\boldsymbol{r},t) = \boldsymbol{B_0}\, e^{i(kz-\omega t)} = \begin{bmatrix} B_{0x}(\boldsymbol{r}) \\ B_{0y}(\boldsymbol{r}) \\ B_{0y}(\boldsymbol{r}) \end{bmatrix} e^{i(kz-\omega t)} \tag{2.63}$$

As $\boldsymbol{E}$ and $\boldsymbol{B}$ satisfies Maxwell's equation in free space, [14] and using $\omega/k = c$, we get,

$$\nabla \cdot \boldsymbol{E} = 0 \tag{2.64}$$

$$\Rightarrow ikE_{0z} + \nabla \cdot \boldsymbol{E_0} = 0 \tag{2.65}$$

$$\nabla \cdot \boldsymbol{B} = 0 \tag{2.66}$$

$$\Rightarrow ikB_{0z} + \nabla \cdot \boldsymbol{B_0} = 0 \tag{2.67}$$

$$\nabla \times \boldsymbol{E} = -\frac{\partial \boldsymbol{B}}{\partial t} \tag{2.68}$$

$$\Rightarrow ik\hat{z} \times \boldsymbol{E_0} + \nabla \times \boldsymbol{E_0} = ikc\boldsymbol{B_0} \tag{2.69}$$

$$\nabla \times \boldsymbol{B} = \frac{1}{c^2}\frac{\partial \boldsymbol{E}}{\partial t} \tag{2.70}$$

$$\Rightarrow ik\hat{z} \times \boldsymbol{B_0} + \nabla \times \boldsymbol{B_0} = -ik\frac{1}{c}\boldsymbol{E_0} \tag{2.71}$$

Assuming paraxial approximation 2.6, we get paraxial wave equation in vector form,

$$\left(\frac{\partial^2}{\partial x^2} + \frac{\partial^2}{\partial y^2} + 2ik\frac{\partial}{\partial z}\right)\begin{Bmatrix} \boldsymbol{E_0} \\ \boldsymbol{B_0} \end{Bmatrix} = 0 \tag{2.72}$$

So each component of $\boldsymbol{E_0}$ and $\boldsymbol{B_0}$ will satisfy the paraxial equation. So,

$$\frac{\partial}{\partial z} = \frac{i}{2k}\left(\frac{\partial^2}{\partial x^2} + \frac{\partial^2}{\partial y^2}\right) \tag{2.73}$$

Now considering slowly varying envelop approximation 2.5 for each component of $\boldsymbol{E_0}$ and $\boldsymbol{B_0}$, from 2.65 and 2.67, we get,

$$E_{0z} = \frac{i}{k}\left(\frac{\partial E_{0x}}{\partial x} + \frac{\partial E_{0y}}{\partial y}\right) \tag{2.74}$$

$$B_{0z} = \frac{i}{k}\left(\frac{\partial B_{0x}}{\partial x} + \frac{\partial B_{0y}}{\partial y}\right) \tag{2.75}$$

Now putting 2.74 in 2.69, and using 2.73, matching $\boldsymbol{B_0}$ component-wise we get,

$$cB_{0x} = -E_{0y} + \frac{1}{2k^2}\left(\frac{\partial^2 E_{0y}}{\partial x^2} - \frac{\partial^2 E_{0y}}{\partial y^2} + 2\frac{\partial^2 E_{0x}}{\partial x \partial y}\right) \tag{2.76}$$

$$cB_{0y} = E_{0x} + \frac{1}{2k^2}\left(\frac{\partial^2 E_{0x}}{\partial y^2} - \frac{\partial^2 E_{0x}}{\partial x^2} - 2\frac{\partial^2 E_{0y}}{\partial x \partial y}\right) \tag{2.77}$$

$$cB_{0z} = \frac{i}{k}\left(\frac{\partial\, cB_{0x}}{\partial x} + \frac{\partial\, cB_{0y}}{\partial y}\right) = \frac{i}{k}\left(\frac{\partial E_{0x}}{\partial y} - \frac{\partial E_{0y}}{\partial x}\right) \tag{2.78}$$

[8]For cylindrical coordinate, ref [16]

Similarly, putting 2.75 in 2.69, and using 2.73, matching $\boldsymbol{E_0}$ component-wise we get,

$$\frac{1}{c}E_{0x} = B_{0y} + \frac{1}{2k^2}\left(\frac{\partial^2 B_{0y}}{\partial x^2} - \frac{\partial^2 B_{0y}}{\partial y^2} - 2\frac{\partial^2 B_{0x}}{\partial x \partial y}\right) \tag{2.79}$$

$$\frac{1}{c}E_{0y} = -B_{0x} + \frac{1}{2k^2}\left(\frac{\partial^2 B_{0x}}{\partial x^2} - \frac{\partial^2 B_{0x}}{\partial y^2} + 2\frac{\partial^2 B_{0y}}{\partial x \partial y}\right) \tag{2.80}$$

$$\frac{1}{c}E_{0z} = \frac{i}{ck}\left(\frac{\partial E_{0x}}{\partial x} + \frac{\partial E_{0y}}{\partial y}\right) = \frac{i}{k}\left(\frac{\partial B_{0y}}{\partial x} - \frac{\partial B_{0x}}{\partial y}\right) \tag{2.81}$$

Let $\psi_x(\boldsymbol{r})$ and $\psi_y(\boldsymbol{r})$ are the dominant x and y component of electric field satisfying paraxial wave equation. If we write magnetic field component as [13]

$$cB_{0x} = -\psi_y + \frac{1}{4k^2}\left(\frac{\partial^2 \psi_y}{\partial x^2} - \frac{\partial^2 \psi_y}{\partial y^2} + 2\frac{\partial^2 \psi_x}{\partial x \partial y}\right) \tag{2.82}$$

$$cB_{0y} = \psi_x + \frac{1}{4k^2}\left(\frac{\partial^2 \psi_x}{\partial y^2} - \frac{\partial^2 \psi_x}{\partial x^2} - 2\frac{\partial^2 \psi_y}{\partial x \partial y}\right) \tag{2.83}$$

$$cB_{0z} = \frac{i}{k}\left(\frac{\partial \psi_x}{\partial y} - \frac{\partial \psi_y}{\partial x}\right) \tag{2.84}$$

and electric field component as [13]

$$E_{0x} = \psi_x + \frac{1}{4k^2}\left(\frac{\partial^2 \psi_x}{\partial x^2} - \frac{\partial^2 \psi_x}{\partial y^2} + 2\frac{\partial^2 \psi_y}{\partial x \partial y}\right) \tag{2.85}$$

$$E_{0y} = \psi_y - \frac{1}{4k^2}\left(\frac{\partial^2 \psi_y}{\partial x^2} - \frac{\partial^2 \psi_y}{\partial y^2} + 2\frac{\partial^2 \psi_x}{\partial x \partial y}\right) \tag{2.86}$$

$$E_{0z} = \frac{i}{k}\left(\frac{\partial \psi_x}{\partial x} + \frac{\partial \psi_y}{\partial y}\right) \tag{2.87}$$

then the eq. 2.82 - 2.87 satisfy the paraxial Maxwell's relations 2.76 - 2.81 up-to the order of $1/(kw_0)^2$, where w_0 is Rayleigh length of Gaussian beam.

Now we will consider two cases of polarization for HG beam - linear and circular polarization.

1. **Linear polarization**
   Let the dominant polarization is in x direction, then $\psi_x = \psi_{m,n}$ of 2.53 and $\psi_y = 0$. The electric field components are

$$E_{0x} = \psi_{m,n} \tag{2.88}$$

$$\begin{aligned} E_{0y} &= \frac{1}{2k^2}\frac{\partial^2 \psi_{m,n}}{\partial x \partial y} \\ &= \frac{1}{4k^2 w_0^2}\left(4mn\psi_{m-1,n-1} - 2m\psi_{m-1,n+1} - 2n\psi_{m+1,n-1} + \psi_{m+1,n+1}\right) \end{aligned} \tag{2.89}$$

$$\begin{aligned} E_{0z} &= \frac{i}{k}\frac{\partial \psi_{m,n}}{\partial x} \\ &= \frac{i}{\sqrt{2}kw_0}\left(2m\psi_{m-1,n} - \psi_{m+1,n}\right) \end{aligned} \tag{2.90}$$

Here we use the the following properties of Hermite polynomials, [23] *i.e.* $\forall x \in \mathbb{R}$ and $\forall n \in \mathbb{N}$,

$$H_{n+1}(x) = 2xH_n(x) - 2nH_{n-1}(x) \tag{2.91}$$

$$\frac{d}{dx}H_n(x) = 2nH_{n-1}(x) \tag{2.92}$$

2. **Circular polarization**
Similarly for LCP, $\psi_x = \psi_{m,n}$ and $\psi_y = i\psi_{m,n}$, the electric field components, using 2.91 and 2.92, are

$$E_{0x} = \frac{1}{\sqrt{2}}\psi_{m,n} \tag{2.93}$$

$$E_{0y} = \frac{i}{\sqrt{2}}\psi_{m,n} \tag{2.94}$$

$$E_{0z} = \frac{i}{2kw_0}\left(4m\psi_{m-1,n} - \psi_{m+1,n} + i2n\psi_{m,n-1} - i\psi_{m,n+1}\right) \tag{2.95}$$

2.9 Relationship between LG & HG modes

According to [24], for $n, m = 0, 1, 2, \dots$

$$\sum_{k=0}^{n+m}(2i)^k\mathcal{P}_k^{(n-k,m-k)}(0)H_{n+m-k}(x)H_k(y) = \begin{cases} 2^{n+m}(-1)^m m!(x+iy)^{n-m}L_m^{n-m}(x^2+y^2), & n \geq m \\ 2^{n+m}(-1)^n n!(x+iy)^{m-n}L_n^{m-n}(x^2+y^2), & m > n \end{cases} \tag{2.96}$$

where

$$\mathcal{P}_k^{(n-k,m-k)}(0) = \frac{(-1)^k}{2^k k!}\frac{d^k}{dt^k}\left[(1-t)^n(1+t)^m\right]\Big|_{t=0} \tag{2.97}$$

Now the scalar field representations of HG and LG beam are

$$U_{m,n}^{HG}(x,y,z) = \frac{C_{m,n}^{HG}}{w(z)}H_m\left(\frac{\sqrt{2}x}{w(z)}\right)H_n\left(\frac{\sqrt{2}y}{w(z)}\right)\exp\left(-\frac{(x^2+y^2)}{w^2(z)}\right)\cdot \exp\left(i\,(m+n+1)\eta - i\frac{k(x^2+y^2)}{2R(z)}\right) \tag{2.98}$$

$$U_{n,m}^{LG}(x,y,z) = (-1)^{\min(n,m)}\frac{C_{m,n}^{LG}}{w(z)}\left[\frac{\sqrt{2(x^2+y^2)}}{w(z)}\right]^{|n-m|}L_{\min(n,m)}^{|n-m|}\left(\frac{2(x^2+y^2)}{w^2(z)}\right)\cdot \exp\left(-\frac{(x^2+y^2)}{w^2(z)}\right)\exp\left(-i(n-m)\arg(x+iy) - i(n+m-1)\eta - i\frac{kr^2}{2R(z)}\right) \tag{2.99}$$

where[9]

$$R(z) = \frac{z_0^2 + z^2}{z} \tag{2.100}$$

$$w(z) = \sqrt{\frac{2(z_0^2 + z^2)}{kz}} \tag{2.101}$$

$$\eta(Z) = \tan^{-1}\left(\frac{z}{z_0}\right) \tag{2.102}$$

and the normalization constants, such that $\iint dx\, dy\, |U| = 1$, are

$$C_{m,n}^{HG} = \sqrt{\frac{2}{\pi n! m!}} 2^{-(m+n)/2} \tag{2.103}$$

$$C_{m,n}^{LG} = \sqrt{\frac{2}{\pi n! m!}} \min(n, m)! \tag{2.104}$$

Here to get the LG beam representation, use $l = n - m$ and $p = \min(n, m)$ in 2.58. [22]

Using the identity 2.96, the LG beam can be decomposed into various order of HG beam by, [20]

$$U_{m,n}^{LG} = \sum_{k=0}^{n+m} i^k b(n, m, k)\, U_{m+n-k,k}^{HG} \tag{2.105}$$

where,

$$b(n, m, k) = \frac{1}{k!} \sqrt{\frac{(n+m)!k!}{2^{n+m} n! m!}} \frac{d^k}{dt^k} \left[(1-t)^n (1+t)^m\right]\Big|_{t=0} \tag{2.106}$$

[9]here $w(z)$ is not the beam half-width but scaled version of that.

3 MOMENTUM OF LIGHT

3.1 Introduction

We know, in addition to its dual nature as waves and particles, EM wave such as light possesses the capability to carries momentum despite its lack of mass. Here we will briefly discuss about different types of momentum carried by EM wave before going to spin-orbit interaction of light in next chapter.

3.2 Linear and angular momentum of light

Momentum carried by EM wave can be two types, linear and angular momentum. The *momentum density* of EM wave is momentum per unit volume.

If linear momentum density is $\boldsymbol{p}$ and linear momentum is $\boldsymbol{P}$ then,

$$\boldsymbol{p} = \frac{1}{c^2}\boldsymbol{S} = \epsilon_0 \boldsymbol{E} \times \boldsymbol{B} \tag{3.1}$$

$$\boldsymbol{P} = \int \boldsymbol{p}\, d\tau \tag{3.2}$$

Now let the monochromatic field with angular frequency ω, then

$$\boldsymbol{\mathcal{E}}(\boldsymbol{r}, t) = \text{Re}\{\boldsymbol{E}(\boldsymbol{r})e^{-i\omega t}\} = \frac{1}{2}(\boldsymbol{E}e^{-i\omega t} + \boldsymbol{E}^* e^{i\omega t}) \tag{3.3}$$

$$\boldsymbol{\mathcal{B}}(\boldsymbol{r}, t) = \text{Re}\{\boldsymbol{B}(\boldsymbol{r})e^{-i\omega t}\} = \frac{1}{2}(\boldsymbol{B}e^{-i\omega t} + \boldsymbol{B}^* e^{i\omega t}) \tag{3.4}$$

From Maxwell-Faraday equation in free space, we know that, [26]

$$\nabla \times \boldsymbol{\mathcal{E}} = -\frac{\partial}{\partial t}\boldsymbol{\mathcal{B}} \tag{3.5}$$

$$\Rightarrow \nabla \times \boldsymbol{E} = i\omega \boldsymbol{B} \tag{3.6}$$

The total energy is given by

$$W = \int d\tau\, \frac{I}{c} = \frac{\epsilon_0}{2} \int d\tau\, \boldsymbol{E}^* \cdot \boldsymbol{E} \tag{3.7}$$

Now time-averaged Poynting vector is given by, [25][26]

$$\langle \boldsymbol{S} \rangle = \frac{1}{\mu_0} \langle \boldsymbol{\mathcal{E}} \times \boldsymbol{\mathcal{B}} \rangle = \frac{1}{\mu_0} \frac{1}{2} \text{Re}\{\boldsymbol{E}^* \times \boldsymbol{B}\} \tag{3.8}$$

From eq. 3.1 and 3.2 and using 3.6 and 3.8, time-averaged linear momentum is given by

$$\boldsymbol{P} = \frac{1}{c^2} \int d\tau\, \langle \boldsymbol{S} \rangle \tag{3.9}$$

$$= \frac{\epsilon_0}{2} \int d\tau\, \text{Re}\{\boldsymbol{E}^* \times \boldsymbol{B}\}$$

$$= \frac{\epsilon_0}{2i\omega} \int d\tau\, \text{Re}\{\boldsymbol{E}^* \times (\nabla \times \boldsymbol{E})\} \tag{3.10}$$

On partial integration and using the transversality of E, considering the magnitude of $\boldsymbol{E}$ decreasing very rapidly when $r \to 0$, [21] we get[10]

$$\boldsymbol{P} = \frac{\epsilon_0}{2i\omega} \int d\tau \left[\sum_{\xi=x,y,z} E_\xi^* \nabla E_\xi \right] \tag{3.11}$$

which is quantum mechanical equivalent for linear momentum of a particle.

Let angular momentum density is $\boldsymbol{j}$ and angular momentum is $\boldsymbol{J}$ then,

$$\boldsymbol{j} = \frac{1}{c^2} \boldsymbol{r} \times \boldsymbol{S} = \epsilon_0 \boldsymbol{r} \times (\boldsymbol{E} \times \boldsymbol{B}) \tag{3.12}$$

$$\boldsymbol{J} = \int \boldsymbol{j}\, d\tau \tag{3.13}$$

Similarly from eq. 3.12 and 3.13 and using 3.6 and 3.8, time-averaged angular momentum,

$$\boldsymbol{J} = \frac{1}{c^2} \int d\tau\, \boldsymbol{r} \times \langle \boldsymbol{S} \rangle \tag{3.14}$$

$$= \frac{\epsilon_0}{2} \int d\tau\, \boldsymbol{r} \times \mathrm{Re}\{\boldsymbol{E}^* \times \boldsymbol{B}\}$$

$$= \frac{\epsilon_0}{2i\omega} \int d\tau\ \mathrm{Re}\{\boldsymbol{r} \times (\boldsymbol{E}^* \times (\nabla \times \boldsymbol{E}))\} \tag{3.15}$$

Now similarly on partial integration and using the transversality of E, considering the magnitude of $\boldsymbol{E}$ decreasing very rapidly when $r \to 0$, [21][22] we get[11]

$$\boldsymbol{J} = \frac{\epsilon_0}{2i\omega} \int d\tau \left[\sum_{\xi=x,y,z} E_\xi^* (\boldsymbol{r} \times \nabla) E_\xi \right] + \frac{\epsilon_0}{2i\omega} \int d\tau \boldsymbol{E}^* \times \boldsymbol{E} \tag{3.16}$$

Now according to [27] & [21], within the paraxial approximation, to get time-averaged energy, linear momentum and angular momentum per unit length *i.e.* $\mathcal{W}$, $\mathcal{P}$ and $\mathcal{J}$ respectively, along the beam propagating in z-direction, we have to integrate throughout the transverse xy-plane. So,

$$\mathcal{W}_z = \frac{\epsilon_0}{2} \iint dx\, dy\, \boldsymbol{E}^* \cdot \boldsymbol{E} \tag{3.17}$$

$$\mathcal{P}_z = \frac{\epsilon_0}{2i\omega} \iint dx\, dy\ \langle \boldsymbol{E} \times (\nabla \times \boldsymbol{E}) \rangle_z \tag{3.18}$$

$$\mathcal{J}_z = \frac{\epsilon_0}{2i\omega} \iint dx\, dy\ [\boldsymbol{r} \times \langle \boldsymbol{E} \times (\nabla \times \boldsymbol{E}) \rangle]_z \tag{3.19}$$

3.3 More on angular momentum

Let the electric field of the paraxial EM wave is [1]

$$\boldsymbol{E}(x, y, z) = \boldsymbol{F}(x, y, z)\, e^{ikz} \tag{3.20}$$

[10] see derivation in Chapter I in ref. [28]
[11] see derivation in Chapter I in ref. [28]

s.t. $\boldsymbol{F}$ is the slowly varying spatial envelop, satisfies the paraxial wave equation 2.6 *i.e.*

$$\nabla_T^2 \boldsymbol{F} + 2ik\frac{\partial \boldsymbol{F}}{\partial r} = 0$$

also assumed that the beam waist w_0 (transverse dimension of the beam) is assumed to be much smaller than the diffraction length, $l_d = kw_0^2$ and z- component of $\boldsymbol{F}$ is smaller than transverse component by a factor of w_0/l_d. [29][21][1]

From previous eq. 3.19, z-component of $\mathcal{J}$ for 3.20 is given by

$$\mathcal{J}_z(z) = \underbrace{\frac{\epsilon_0}{2i\omega}\iint dx\,dy\,\left[F_\xi^*\left(x\frac{\partial}{\partial y} - y\frac{\partial}{\partial x}\right)F_\xi\right]_{\xi=x,y}}_{\text{1st term}} + \underbrace{\frac{\epsilon_0}{2i\omega}\iint dx\,dy\,(F_x^* F_y + F_y^* F_x)}_{\text{2nd term}} \tag{3.21}$$

Note that, in 3.21, we can separately identify two terms. According to [1], the first is associated with transverse distribution of electric field (amplitude and phase) as $x\frac{\partial}{\partial y} - y\frac{\partial}{\partial x}$ is equivalent to $\frac{\partial}{\partial \phi}$ in cylindrical coordinate and the second term to the polarization of electric field. Thus it is concluded,[21] within the paraxial approximation, that

1. first term is the orbital angular momentum (OAM) per unit length in z of the EM wave,

$$\begin{aligned}\mathcal{L} &= \frac{\epsilon_0}{2i\omega}\iint dx\,dy\,\left[F_\xi^*\left(x\frac{\partial}{\partial y} - y\frac{\partial}{\partial x}\right)F_\xi\right]_{\xi=x,y} \\ &= \frac{\epsilon_0}{2i\omega}\iint dx\,dy\,\left[F_\xi^*\left(\boldsymbol{r}\times\nabla\right)_z F_\xi\right]_{\xi=x,y}\end{aligned} \tag{3.22}$$

   which is quantum mechanical equivalent of z-component of the angular momentum of a particle.

2. second term is the spin angular momentum (SAM) per unit length in z,

$$\mathcal{S} = \frac{\epsilon_0}{2i\omega}\iint dx\,dy\,(F_x^* F_y + F_y^* F_x) \tag{3.23}$$

3.3.1 Orbital and spin Angular Momentum

Let envelop $\boldsymbol{F}$ corresponding to the EM wave 3.20 for a vortex beam (*e.g.* LG beam) be,

$$\boldsymbol{F}(r,\phi) = u(r)\,\exp(-il\phi)\,\hat{\boldsymbol{p}} \tag{3.24}$$

where $e^{il\phi}$ refers to helical phase front, and $\hat{\boldsymbol{p}} = p_x\hat{x} + p_y\hat{y} + p_z\hat{z}$ refers to unit polarization direction of electric field. Putting it in 3.22 considering $x\frac{\partial}{\partial y} - y\frac{\partial}{\partial x} \equiv \frac{\partial}{\partial \phi}$, we get,

$$\begin{aligned}\mathcal{L} &= \frac{\epsilon_0}{2i\omega}\iint r\,dr\,d\phi\,\left[F_\xi^*\frac{\partial}{\partial \phi}F_\xi\right]_{\xi=x,y} \\ &= \frac{\epsilon_0}{2\omega}l\left(|p_x|^2 + |p_y|^2\right)2\pi\int r\,dr\,|u(r)|^2\end{aligned}$$

considering z-component of $\hat{\boldsymbol{p}}$ is smaller than transverse component by a factor of w_0/l_d, so $|p_x|^2 + |p_y|^2 \approx |p_x|^2 + |p_y|^2 + |p_z|^2 = |\hat{\boldsymbol{p}}|^2 = 1$, then

$$\mathcal{L} = \frac{\pi \epsilon_0 l}{\omega} \int r\, dr\, |u(r)|^2 \tag{3.25}$$

For the SAM part 3.23,

$$\begin{aligned}\mathcal{S} &= \frac{\epsilon_0}{2i\omega} \iint r\, dr\, d\phi\, (F_x^* F_y + F_y^* F_x) \\ &= \frac{\epsilon_0}{2i\omega} (p_x^* p_y - p_y^* p_x) 2\pi \int r\, dr\, |u(r)|^2 \end{aligned}\tag{3.26}$$

Define *polarization helicity*, σ as

$$\sigma = 2\,\mathrm{Im}(p_x^*\, p_y) = \frac{1}{i}(p_x^* p_y - p_y^* p_x) \tag{3.27}$$

then

$$\mathcal{S} = \frac{\pi \epsilon_0 \sigma}{\omega} \int r\, dr\, |u(r)|^2 \tag{3.28}$$

The relation[12] between polarization direction $\hat{\boldsymbol{p}}$ and normalized Jones vector $\boldsymbol{J}$ is $\hat{\boldsymbol{p}} = \boldsymbol{J} e^{i\delta}$, for some phase difference δ.

So

$$\sigma = \frac{1}{i}(p_x^* p_y - p_y^* p_x) = \frac{1}{i}(J_x^* J_y - J_y^* J_x) \tag{3.29}$$

Using table 1,

1. For LCP, $\sigma = \frac{1}{2i}(1i + 1i) = 1$
2. For RCP, $\sigma = \frac{1}{2i}(-1i - 1i) = -1$
3. for linearly polarized, $\sigma = \frac{1}{i}(1 - 1) = 0$, so no SAM.

Now for $\mathcal{W}$ in 3.17, we get,

$$\begin{aligned}\mathcal{W}_z &= \frac{\epsilon_0}{2} \iint r\, dr\, d\phi\, \boldsymbol{E}^* \cdot \boldsymbol{E} \\ &= \frac{\epsilon_0}{2} \iint r\, dr\, d\phi\, \boldsymbol{F}^* \cdot \boldsymbol{F} \\ &= \frac{\epsilon_0}{2} \left(|p_x|^2 + |p_y|^2 + |p_z|^2 \right) 2\pi \int r\, dr\, |u(r)|^2 \\ &= \pi \epsilon_0 \int r\, dr\, |u(r)|^2 \end{aligned}\tag{3.30}$$

See from 3.25 and 3.30,

$$\frac{\mathcal{L}}{\mathcal{W}_z} = \frac{l}{\omega} = \frac{\text{OAM}}{\text{Total energy}} \tag{3.31}$$

[12] for polarized light only

from 3.28 and 3.30,

$$\frac{\mathcal{S}}{\mathcal{W}_z} = \frac{\sigma}{\omega} = \frac{\text{SAM}}{\text{Total energy}} \tag{3.32}$$

and from 3.31 and 3.32,

$$\frac{\mathcal{J}_z}{\mathcal{W}_z} = \frac{\mathcal{L}+\mathcal{S}}{\mathcal{W}_z} = \frac{l+\sigma}{\omega} = \frac{\text{Total AM}}{\text{Total energy}} \tag{3.33}$$

We know for a photon the energy associated with it is $\hbar\omega$, then from 3.31 and 3.32, we can say, the OAM associated with one photon of paraxial vortex beam is $l\hbar$ and SAM associated with one photon is $\sigma\hbar$.

3.3.2 Intrinsic and Extrinsic nature of angular momentum

If we observe the expression of $\mathcal{J}_z$ in 3.19, it may depends on the choice of the axis (usually $\boldsymbol{r} = (0,0)$), from which we measure $\boldsymbol{r}$. [1][30] But if we shift the $\boldsymbol{r}$ *s.t.*

$$\boldsymbol{r} \longrightarrow \boldsymbol{r'} = \boldsymbol{r} + \boldsymbol{r_0} \tag{3.34}$$

$$(x,y) \longrightarrow (x',y') = (x,y) + (x_0,y_0) \tag{3.35}$$

then change of $\mathcal{J}_z$ will be

$$\mathcal{J}_z \longrightarrow \mathcal{J'}_z = \mathcal{J}_z + (\boldsymbol{r_0} \times \mathcal{P}) \cdot \hat{z} \tag{3.36}$$

The change in angular momentum,

$$\Delta\mathcal{J}_z = \mathcal{J'}_z - \mathcal{J}_z = (\boldsymbol{r_0} \times \mathcal{P}) \cdot \hat{z} \tag{3.37}$$

$$\Rightarrow \Delta\mathcal{J}_z = \frac{x_0\epsilon_0}{2} \iint dx\, dy\, \langle \boldsymbol{E} \times \boldsymbol{B} \rangle_y + \frac{y_0\epsilon_0}{2} \iint dx\, dy\, \langle \boldsymbol{E} \times \boldsymbol{B} \rangle_x \tag{3.38}$$

Now, we say the AM is *intrinsic*, when the AM does not depends on the choice of the reference axis, and *extrinsic* when it depends on the choice of axis.

If the AM is to be intrinsic, then for all (x_0, y_0)

$$\Delta\mathcal{J} = 0$$
$$\Rightarrow \iint dx\, dy\, \langle \boldsymbol{E} \times \boldsymbol{B} \rangle_y = 0 = \iint dx\, dy\, \langle \boldsymbol{E} \times \boldsymbol{B} \rangle_x \tag{3.39}$$

From the SAM part, we see $\mathcal{S}$ does not depend on the choice of the axis, so SAM is intrinsic. But for the OAM part, we see $\mathcal{L}$ depends on the choice of the axis, so OAM may be intrinsic or extrinsic determined by, (from 3.22)

$$\Delta\mathcal{L} = \iint dx\, dy\, \left[F_\xi^* \left(\boldsymbol{r_0} \times \nabla\right)_z F_\xi\right] = 0, \text{ where } \xi = x, y \tag{3.40}$$

4 SPIN-ORBIT INTERACTION

4.1 Introduction

The interaction between light and matter is a fascinating realm of physics. One crucial of this interaction is the spin-orbit interaction on light. The underlying framework is the interaction between the spin and orbital angular momentum of light. In this section, we will briefly discuss about that.

4.2 Spin-orbit energy

In quantum mechanics, spin-orbit interaction is a common phenomena. We can see it in the splitting of spectral lines into fine structure. For a simple case like H atom, a electron in orbit around the nucleus, the spin-orbit coupling results from the interaction between electron's spin magnetic moment and nucleus's orbital magnetic field, which we will discuss below. [1][31]

The spin magnetic moment of a electron is given by

$$\boldsymbol{\mu_s} = -\frac{e}{m_e c}\boldsymbol{S} \tag{4.1}$$

where e, m_e are absolute charge and mass of electron respectively and $\boldsymbol{S}$ is spin angular momentum of electron.

For our system, the electric field is centrally symmetric *i.e.*

$$\boldsymbol{E} = -\frac{1}{e}\frac{dU}{dr}\hat{\boldsymbol{r}} = -\frac{1}{er}\frac{dU}{dr}\boldsymbol{r} \tag{4.2}$$

where U is the potential energy,

$$U = \frac{1}{4\pi\epsilon_0}\frac{e^2}{r} \tag{4.3}$$

Now if electron rotates around the nucleus with instantaneous velocity $\boldsymbol{v}$, then from the rest frame of electron, the nucleus is rotating with $-\boldsymbol{v}$ around the electron thus creating a magnetic field in centre, which is[13]

$$\boldsymbol{B} = -\frac{1}{c}\boldsymbol{v}\times\boldsymbol{E} = -\frac{1}{m_e c}\boldsymbol{E}\times\boldsymbol{P} \tag{4.4}$$

where $\boldsymbol{P} = m_e\boldsymbol{v}$ is momentum.

Due to spin-orbit interaction, the corresponding interaction energy rises,

$$H_{so} = -\boldsymbol{\mu_s}\cdot\boldsymbol{B} = -\frac{e}{m_e c}\boldsymbol{S}\cdot\boldsymbol{B} = -\frac{e}{m_e^2c^2}\boldsymbol{S}\cdot(\boldsymbol{E}\times\boldsymbol{P}) = \frac{1}{m_e^2c^2 r}\frac{dU}{dr}\boldsymbol{S}\cdot(\boldsymbol{r}\times\boldsymbol{P}) \tag{4.5}$$

Taking orbital angular momentum $\boldsymbol{L} = \boldsymbol{r}\times\boldsymbol{P}$, we get,

$$H_{so} = \frac{1}{m_e^2c^2 r}\frac{dU}{dr}\boldsymbol{S}\cdot\boldsymbol{L} \tag{4.6}$$

We call H_{so} as *Spin-orbit energy.*[14]

[13] the coefficient $1/c$ is in cgs, but $1/c^2$ in SI. [32]

[14] By Thomas precision, multiplication of a factor of $1/2$ is necessary to agree with experimental results. It is informally known as the "Thomas half". [33]

4.3 Geometric phase of light

We know from the knowledge of waves, there is the phase factor corresponding to the EM wave due to optical path length difference, called *dynamical phase*. But there is another phase factor other than dynamical one, due to the geometry or topology of the evolution of the electromagnetic wave, we call it *Geometric phase*.[1] Geometric phases arises from intrinsic angular momentum and rotations of coordinates. The geometric phase and angular momentum underlie the SOI of light.[39] The two types of geometric phases, will be discussed, are

1. Spin-redirection Berry phase
2. Pancharatnam-Berry phase

4.3.1 Spin-redirection Berry phase

This *Berry phase* associated with adiabatic evolution of wave-vector $\boldsymbol{k}$. When the wave vector complete a adiabatic cycle, we will find a geometric phase arises from it. As an example, let a polarized light passes through a helical optic fibre with very low (negligible) birefringence and no torsional stress[15]. After one helical patch, the $\boldsymbol{k}$ wave-vector come to the same state, but gives rise of a helicity-dependant geometric phase[16] called *spin-redirection Berry phase*. [39]

For circularly polarized light, we can write Jones vector as

$$\boldsymbol{J} = \begin{bmatrix} 1 \\ i\sigma \end{bmatrix} \tag{4.7}$$

where σ is helicity (either $+1$ or -1).

Considering transversality of electric field, it will be tangent on the sphere in momentum space. And in one adiabatic cycle of wave-vector *w.r.t.* k_z, the non-trivial parallel transport of the electric-field vectors takes place on the sphere.[39] So after transportation of a vector, the vector is rotated by an angle Θ [35] *i.e.* the frame is rotated by an angle Θ where

$$\Theta = 2\pi(1 - \cos\theta) \tag{4.8}$$

where θ is half-apex angle of the cone formed by sweeping the wave vector $\boldsymbol{k}$ in momentum space (see fig 15b). Note that Θ is the solid angle obtained at the apex of the cone.

After one adiabatic cycle, electric field vector for circularly polarized light, $\boldsymbol{J}$ transform into $\boldsymbol{J'}$ where

$$\boldsymbol{J} \longrightarrow \boldsymbol{J'} = \boldsymbol{J}\exp(i\Theta_G) \tag{4.9}$$

where Θ_G is the acquired helicity-dependant geometric phase *s.t.*

$$\Theta_G = \sigma\Theta \tag{4.10}$$

So,

$$|L\rangle \longrightarrow e^{i\Theta}|L\rangle \tag{4.11}$$

$$|R\rangle \longrightarrow e^{-i\Theta}|R\rangle \tag{4.12}$$

[15] Torsional stress produces circular birefringence by elasto-optic effect. [37]

[16] This is a non-holonomic process *i.e.* the final state depends on the path taken by the system. [34]

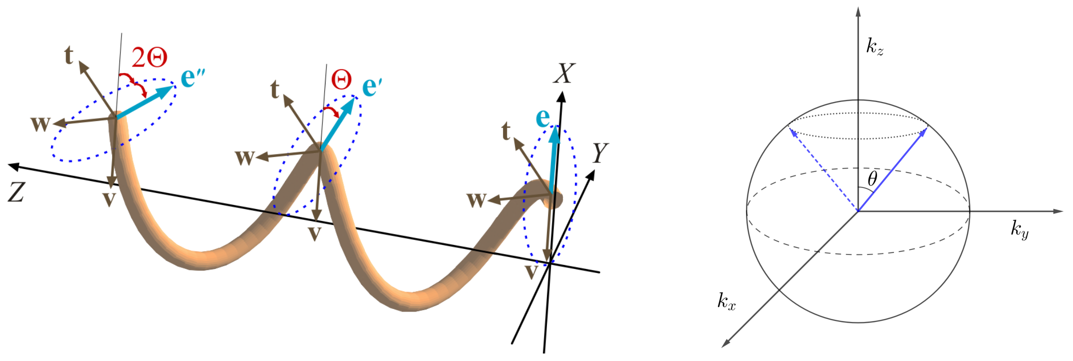

(a) Evolution of polarization axis along helical optic fibre (ref. [38])

(b) Evolution of wave-vector $\boldsymbol{k}$ along helical optic fibre in momentum space

Figure 15: Geometric Berry phase arises along helical optic fibre

Now for x-polarized light, $|x_{in}\rangle$ and $|x_{out}\rangle$ will be

$$|x_{in}\rangle = \frac{1}{\sqrt{2}} (|L\rangle + |R\rangle) \tag{4.13}$$

$$|x_{out}\rangle = \frac{1}{\sqrt{2}} \left(e^{i\Theta} |L\rangle + e^{-i\Theta} |R\rangle\right) \tag{4.14}$$

So the x-polarized light is rotated by angle Θ after one cycle, shown in fig 15a. Note that θ does not originate from intrinsic anisotropy and it is geometric one. We call it *spin-redirection Berry phase.*

4.3.2 Pancharatnam-Berry Phase

Unlike the previous one, the *Pancharatnam-Berry phase* arises after a cyclic evolution in Poincare sphere when the state of polarization changes keeping wave-vector $\boldsymbol{k}$ is fixed. Convenient example of observation of Pancharatnam-Berry phase is Michelson interferometer setup, (see fig. 16) in which one arm of the interferometer has two quarter wave-plates, one (QP1) is fixed and another one (QP2) is rotatable. [40]

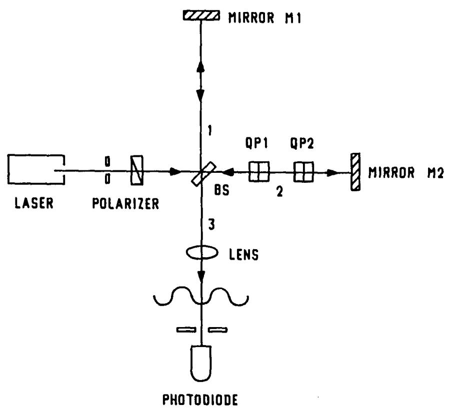

Figure 16: Schematic of Michelson interferometer setup for observation of Pancharatnam-Berry phase (ref. [40])

Fast axis of QP1 and QP2 are aligned at $\theta_1 = \pi/4$ and $\theta_2 = \beta$ *w.r.t.* x-axis, respectively. The input light is x-polarized. Then the polarization state of output light at different part of arm 2 in Michelson interferometer is shown in fig 17, and corresponding Jones calculus shown in table 5.

Poincare Sphere point (pol. state)	Polarization state (Jones vector, $\boldsymbol{J}$)
A ($\|A\rangle$)	$\boldsymbol{J}_A = \begin{bmatrix}1\\0\end{bmatrix}$
R ($\|R\rangle$)	$\boldsymbol{J}_R = R(-\pi/4)\, \boldsymbol{M}_{QP}\, R(\pi/4)\, \boldsymbol{J}_A = \frac{e^{i\phi'}}{2}\begin{bmatrix}1+i & 1-i\\1-i & 1+i\end{bmatrix}\begin{bmatrix}1\\0\end{bmatrix}$ $= \frac{e^{i\phi'}}{2}\begin{bmatrix}1+i\\1-i\end{bmatrix} = \frac{1}{\sqrt{2}}\begin{bmatrix}1\\-i\end{bmatrix}\exp(i\phi_1)$
B ($\|B\rangle$)	$\boldsymbol{J}_B = R(-\beta)\, \boldsymbol{M}_{QP}\, R(\beta)\, \boldsymbol{J}_R$ $= e^{i\phi''}\begin{bmatrix}\cos^2(\beta)+i\sin^2(\beta) & (1-i)\sin(\beta)\cos(\beta)\\(1-i)\sin(\beta)\cos(\beta) & \sin^2(\beta)+i\cos^2(\beta)\end{bmatrix}\frac{1}{\sqrt{2}}\begin{bmatrix}1\\-i\end{bmatrix}\exp(i\phi_1)$ $= \begin{bmatrix}\cos(\beta+\pi/4)\\\sin(\beta+\pi/4)\end{bmatrix}\exp(i\phi_2)\ \exp(-i\beta)$ $= \begin{bmatrix}\cos(\varphi)\\\sin(\varphi)\end{bmatrix}\exp(i\phi_3)\,\exp(-i\varphi)$ where $\varphi = \beta + \pi/4$
C ($\|C\rangle$)	$\boldsymbol{J}_C = \boldsymbol{M}_{Mirror}\, \boldsymbol{J}_B = e^{i\pi}\begin{bmatrix}-1 & 0\\0 & 1\end{bmatrix}\begin{bmatrix}\cos(\varphi)\\\sin(\varphi)\end{bmatrix}\exp(i\phi_3)\,\exp(-i\varphi)$ $= \begin{bmatrix}-\cos(\varphi)\\\sin(\varphi)\end{bmatrix}\exp(i\phi_4)\,\exp(-i\varphi)$
L ($\|L\rangle$)	$\boldsymbol{J}_L = \begin{bmatrix}1\\i\end{bmatrix}\exp(i\phi_5)\,\exp(-i\,2\varphi)$
A ($\|A'\rangle$)	$\boldsymbol{J}'_A = \begin{bmatrix}1\\0\end{bmatrix}\exp(i\phi_6)\,\exp(-i\,2\varphi)$ $= \boldsymbol{J}_A\exp(i\phi_6)\,\exp(-i\,2\varphi)$

Table 5: Jones vector of polarization state in Pancharatnam-Berry phase

We see that the light with linear polarization state ($|B\rangle$) acquired a additional phase term *i.e.* $\exp(-i\,2\varphi)$ which only depends on orientation of fast axis of QP2 *i.e.* $\varphi = \beta + \pi/4$ and does not depend on thickness and refractive index of the birefringent wave-plate, so this phase is purely geometric one. Other all ϕ's are all dynamical phase factors. [1]

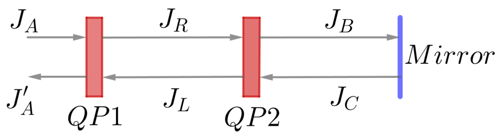

(a) Michelson interferometer arm 2

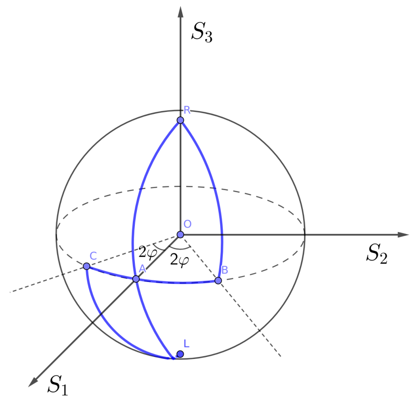

(b) Corresponding cyclic evolution in Poincare sphere

Figure 17: Evolution of polarization state in arm 2

We see after one cyclic evolution in Poincare sphere in path ARBCLA,

$$|A\rangle \longrightarrow |A'\rangle = |A\rangle \exp(i\phi_6 - i\,2\varphi) \tag{4.15}$$

So at photodiode the intensity variation *w.r.t.* β will be

$$\begin{aligned} I &= (\langle A| + \langle A'|)(|A\rangle + |A'\rangle) \\ &= \langle A|A\rangle\,(1 + \exp(-i\phi_6 + i2\varphi))\,(1 + \exp(i\phi_6 - i2\varphi)) \\ &= \langle A|A\rangle\,(2 + 2\cos(2\varphi - \phi_6)) \\ \Rightarrow I(\beta) &= 2\,\langle A|A\rangle\,(1 - \sin(2\beta - \phi_6)) \end{aligned} \tag{4.16}$$

Experimental verification by Chyba *et al* (ref. [40]) is given in figure 18.

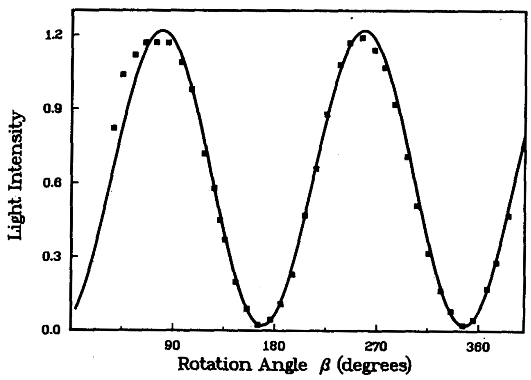

(a) Measured intensity vs Rotation angle β of QP2, fitted with eq. 4.16

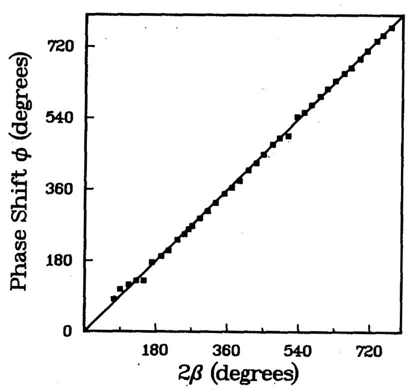

(b) Measured phase shift vs rotation angle β, with solid line of $\phi = 2\beta$

Figure 18: Measurement of the Pancharatnam phase by Chyba *et al* (ref. [40])

4.3.3 Rotational frequency shift of light

Rotational frequency shift is the dynamical manifestation of Pancharatnam-Berry Phase. Let there is half wave-plate rotating *w.r.t.* centre axis at Ω. If the alignment of the fast axis of half wave-plate is θ, then

$$\Omega = \frac{d\theta}{dt} \tag{4.17}$$

$$\theta = \Omega t \tag{4.18}$$

let the Jones electric field vector of input light is

$$\boldsymbol{E}_{in} = \frac{1}{\sqrt{2}}\begin{bmatrix}1\\ i\sigma\end{bmatrix} \tag{4.19}$$

then the Jones electric field vector of output light is

$$\begin{aligned}\boldsymbol{E}_{out}(\theta) &= R(-\theta)\boldsymbol{M}_{\lambda/2}R(\theta)\boldsymbol{E}_{in} = R(-\theta)\begin{bmatrix}1 & 0\\ 0 & -1\end{bmatrix}R(\theta)\boldsymbol{E}_{in}\\ &= \begin{bmatrix}\cos(2\theta) & \sin(2\theta)\\ \sin(2\theta) & -\cos(2\theta)\end{bmatrix}\frac{1}{\sqrt{2}}\begin{bmatrix}1\\ i\sigma\end{bmatrix} = \frac{1}{\sqrt{2}}\begin{bmatrix}1\\ -i\sigma\end{bmatrix}\exp(i2\sigma\theta)\\ \Rightarrow \boldsymbol{E}_{out}(t) &= \frac{1}{\sqrt{2}}\begin{bmatrix}1\\ -i\sigma\end{bmatrix}\exp(i2\sigma\Omega t)\end{aligned} \tag{4.20}$$

If angular frequency of the input beam is ω, then the angular frequency of output beam be $(\omega + 2\sigma\Omega)$. So change in angular frequency, $\Delta\omega = 2\sigma\Omega$. This is spin-dependant *rotational Doppler shift* of SAM carrying light beam. [1]

4.4 Types of SOI

We have discussed brief of angular momentum of light in previous chapter. The different types of angular momentum a EM beam carries are

1. Spin AM ($\boldsymbol{S}$) or SAM
2. Intrinsic orbital AM ($\boldsymbol{L}_{int}$) or IOAM
3. Extrinsic orbital AM ($\boldsymbol{L}_{ext}$) or EOAM

SAM is associated with degree of circular polarization and also intrinsic in nature. The IOAM is associated with the optical vortex structure of the beam (*e.g.* vortex beam like LG beam), so it is intrinsic. Whereas the EOAM is associated with the trajectory of centroid of the beam. [41] (see fig 19)

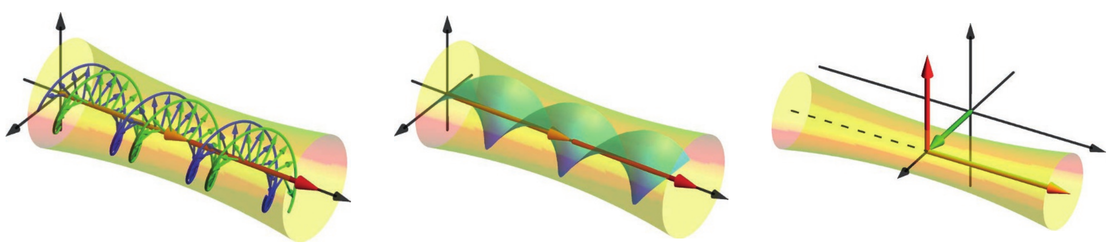

(a) SAM of RCP beam of $\sigma = -1$

(b) Intrinsic OAM of vortex beam of $l = 2$

(c) Extrinsic OAM of beam at $\boldsymbol{R}$ away from origin

Figure 19: Angular momentum of paraxial beam, yellow arrow denotes linear momentum and red arrow denotes angular momentum (ref. [39])

The inter-conversion between these different angular momentum in a process represents *spin-orbit interaction* of light. [39] The three type of interaction are

1. between $\boldsymbol{S}$ and $\boldsymbol{L}_{int}$
2. between $\boldsymbol{S}$ and $\boldsymbol{L}_{ext}$
3. between $\boldsymbol{L}_{int}$ and $\boldsymbol{L}_{ext}$

In the later section, we will see several manifestation of those interactions.

4.5 SOI in anisotropic medium

Inhomogeneous anisotropic medium has spatially varying anisotropy axis (*i.e.* birefringent or dichroic. Here SOI deals with spin flipping, spin-to-orbital angular momentum conversion etc. To illustrate these events, we will consider specific cases.

A simple case of homogenous medium is when a circularly polarized light passes through quarter wave-plate, it become linearly polarized light, so the SAM transformation is

$$\sigma = \pm 1 \longrightarrow \sigma = 0$$

In that case, $\pm\hbar$ SAM carried by each photon of circularly polarized light, is transferred to the wave plate. Similarly for half wave-plate, the SAM transformation is

$$\sigma = \pm 1 \longrightarrow \sigma = \mp 1$$

So the spin is flipped.

Before going into more complex cases, we discuss about *q-plate*. Q-plate is an birefringent anisotropic media of specific phase retardation across the slab with an inhomogeneous orientation of the fast (or slow) optical axis lying parallel to the slab planes whose local alignment of birefringent fast axis varies linearly with the azimuth angle of the q-plate. [42] Let local alignment angle is α, and the azimuth angle is ϕ, then,

$$\alpha(\phi) = q\phi + \alpha_0 \tag{4.21}$$

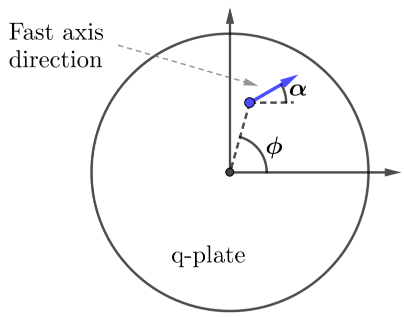

Figure 20: local birefringent fast axis alignment in q-plate

Now the corresponding Jones matrix at each point of the q-plate of phase retardation of π, will be [42]

$$\begin{aligned}\boldsymbol{M}_q(\phi) &= R(-\alpha)\boldsymbol{M}_{\lambda/2}R(\alpha) = R(-\alpha)\begin{bmatrix}1 & 0\\ 0 & -1\end{bmatrix}R(\alpha)\\ &= \begin{bmatrix}\cos(2\alpha) & \sin(2\alpha)\\ \sin(2\alpha) & -\cos(2\alpha)\end{bmatrix}\end{aligned} \tag{4.22}$$

Let considering transversal of electric field, for each ray of a paraxial beam of circular polarization ($\sigma = \pm 1$) the Jones electric field is

$$\boldsymbol{E}_{in} = \frac{1}{\sqrt{2}}\begin{bmatrix}1\\ i\sigma\end{bmatrix} \tag{4.23}$$

then the output electric filed vector will be

$$\boldsymbol{E}_{out}(\phi) = \boldsymbol{M}_q(\phi)\frac{1}{\sqrt{2}}\begin{bmatrix}1\\ i\sigma\end{bmatrix} = \exp(i2\sigma\alpha)\frac{1}{\sqrt{2}}\begin{bmatrix}1\\ -i\sigma\end{bmatrix} = \frac{1}{\sqrt{2}}\begin{bmatrix}1\\ -i\sigma\end{bmatrix}\exp(i2\sigma q\phi)\ \exp(i2\sigma\alpha_0) \tag{4.24}$$

So the output beam has spin flipping. Moreover the beam has acquired a spin-dependant phase factor $\exp(i2\sigma q\phi)$, which makes it a vortex beam. From 3.31 we see that output light carries $2q\hbar$ angular momentum per photon. Here the change of angular momentum is

$$(\sigma = \pm 1, l = 0) \longrightarrow (\sigma = \mp 1, l = \pm 2q)$$

So to keep total angular momentum per photon conserved, $q = 1$.

Now let the q-plate is of phase retardation of $\pi/2$, then

$$\begin{aligned}\boldsymbol{M}_q(\phi) &= R(-\alpha)\boldsymbol{M}_{\lambda/4}R(\alpha) = R(-\alpha)\begin{bmatrix}1 & 0\\ 0 & i\end{bmatrix}R(\alpha)\\ &= \begin{bmatrix}\cos^2(\alpha) + i\sin^2(\alpha) & (1-i)\sin(\alpha)\cos(\alpha)\\ (1-i)\sin(\alpha)\cos(\alpha) & \sin^2(\alpha) + i\cos^2(\alpha)\end{bmatrix}\end{aligned} \tag{4.25}$$

Putting circularly polarized light (as in Pancharatnam-Berry phase, see table 5), electric filed vector will be

$$\begin{aligned}\boldsymbol{E}_{out}(\phi) &= \boldsymbol{M}_q(\phi)\frac{1}{\sqrt{2}}\begin{bmatrix}1\\ i\sigma\end{bmatrix} = \exp(i\sigma\alpha)\begin{bmatrix}\cos(\alpha - \sigma\pi/4)\\ \sin(\alpha - \sigma\pi/4)\end{bmatrix}\\ &= \begin{bmatrix}\cos(\alpha - \sigma\pi/4)\\ \sin(\alpha - \sigma\pi/4)\end{bmatrix}\exp(i\sigma q\phi)\ \exp(i\sigma\alpha_0)\end{aligned} \tag{4.26}$$

So the output beam has a phase factor $\exp(i\sigma q\phi)$. Here the change of angular momentum is

$$(\sigma = \pm 1, l = 0) \longrightarrow (\sigma = 0, l = \pm q)$$

So to keep total angular momentum per photon conserved, $q = 1$.

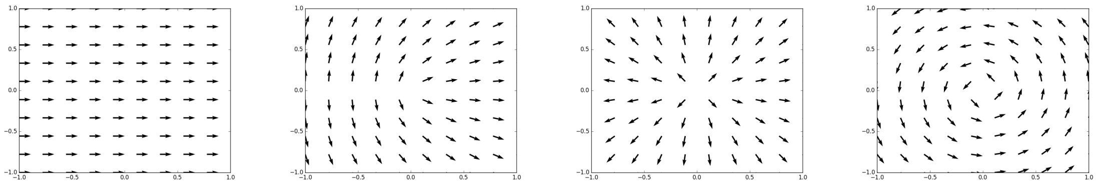

(a) $q = 0,\ \alpha_0 = 0$ (b) $q = 0.5,\ \alpha_0 = 0$ (c) $q = 1,\ \alpha_0 = 0$ (d) $q = 1,\ \alpha_0 = \pi/2$

Figure 21: Q-plate of different q and α_0

Now we will discuss about the diffractive optical element, especially computer-generated hologram (CGH). Its advantage is that, it can mimic any refractive element of choice, but only for at a single wavelength. To produce helical phase front, CHG (forked diffraction gratings or spiral Fresnel lenses, see fig 22,23) is used which is combination of helical phase hologram and linear phase ramp[17] with modulo 2π. [43]

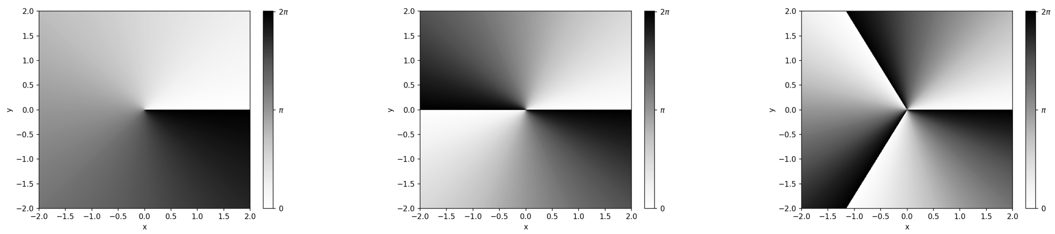

(a) $l = 1$ (b) $l = 2$ (c) $l = 3$

Figure 22: Helical phase hologram for different values of l

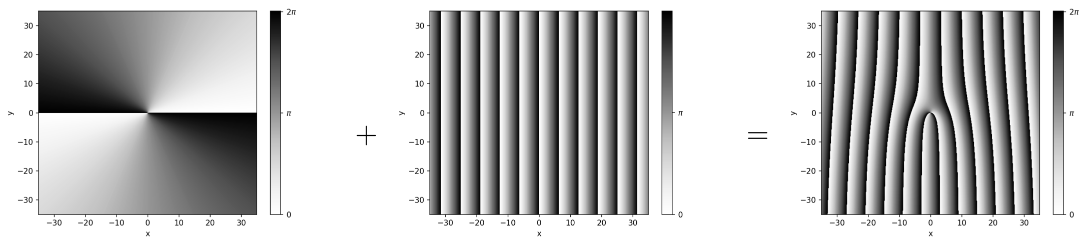

(a) Helical phase (b) Linear phase (c) Forked phase

Figure 23: CHG used to generate helical phase front

If input beam, $\boldsymbol{J}_{in}$ of planer phase front passes through the CGH given fig 23c), then output beam is $\boldsymbol{J}_{out}$ *s.t.*,

$$\boldsymbol{J}_{out} = \boldsymbol{J}_{in} \exp(il\phi) \tag{4.27}$$

which has helical phase structure resulting non-zero OAM. So change in OAM is,

$$(l = 0) \longrightarrow (l = l)$$

[17] Linear phase ramp is used to deviate the beam from the former propagation axis. [44]

So, per photon $l\hbar$ OAM is transferred to CGH. Further, this can be used in beam shaping, wavefront shaping, LG-HG beam transformation etc. [43][22]

References

[1] Gupta, S.D., Ghosh, N., & Banerjee, A. (2015). Wave Optics: Basic Concepts and Contemporary Trends (1st ed.). CRC Press. doi:10.1201/b19330

[2] Born, Max; Wolf, Emil (1999). Principles of optics: electromagnetic theory of propagation, interference and diffraction of light (7th expanded ed.). Cambridge: Cambridge University Press. ISBN 0-521-64222-1. OCLC 1151058062

[3] Jones Calculus - Wikipedia

[4] Wang Jizhong (1986). A matrix method for describing unpolarized light and its applications. , 2(4), 362-372. doi:10.1007/bf02488478

[5] Simon, B. N.; Simon, S.; Mukunda, N.; Gori, F.; Santarsiero, M.; Borghi, R.; Simon, R. (2010). A complete characterization of pre-Mueller and Mueller matrices in polarization optics. josaa/27/2/josaa-27-2-188.pdf, 27(2), 188-0. doi: 10.1364/JOSAA.27.000188

[6] Hecht, Eugene (1970). Note on an Operational Definition of the Stokes Parameters. American Journal of Physics, 38(9), 1156-. doi: 10.1119/1.1976574

[7] Collett E. (2005). Field guide to polarization. SPIE Press.

[8] Goldstein, D.H. (2011). Polarized Light (3rd ed.). CRC Press. doi: 10.1201/b10436

[9] Milonni, P.W. and Eberly, J.H. (2010). Laser Physics. Wiley & Sons, Hoboken, Chapter 7. doi: 10.1002/9780470409718

[10] Lasers and Optoelectronics: ECE 4300 Cornell University

[11] Kogelnik, H., & Li, T. (1966). Laser beams and resonators. Applied optics, 5(10), 1550-1567.

[12] Optical cavity - Wikipedia

[13] Erikson, W. L.; Singh, S. (1994). Polarization properties of Maxwell-Gaussian laser beams. Physical Review E, 49(6), 5778-5786. doi: 10.1103/PhysRevE.49.5778

[14] Maxwell's equations - Wikipedia

[15] Conry, J. P. (2012). Polarization Properties of Maxwell-Gauss Laser Beams. Graduate Theses and Dissertations Retrieved from https://scholarworks.uark.edu/etd/491.

[16] Lewis, W. E.; Vyas, R. (2014). Maxwell-Gaussian beams with cylindrical polarization. Journal of the Optical Society of America A, 31(7), 1595-. doi: 10.1364/josaa.31.001595

[17] Normal distribution - Wikipedia

[18] Introduction of Gaussian Beam - Tohoku University

[19] Andrews, D., & Babiker, M. (Eds.). (2012). The Angular Momentum of Light. Cambridge: Cambridge University Press. doi: 10.1017/CBO9780511795213

[20] MW Beijersbergen, L Allen, H Van der Veen, and JP Woerdman (1993). Astigmatic laser mode converters and transfer of orbital angular momentum. Opt. Commun., 96(1):123-132.

[21] S.J. van Enk; G. Nienhuis (1992). Eigenfunction description of laser beams and orbital angular momentum of light. 94(1-3), 147-158. doi: 10.1016/0030-4018(92)90424-p

[22] Allen, L. (1999).The Orbital Angular Momentum of Light. Progress in Optics. Volume 39. 291-372. doi: 10.1016/S0079-6638(08)70391-3

[23] Lebedev, N. N. (1972), Special Functions and Their Applications, Dover Publications Inc.

[24] Abramochkin, E. and Volostnikov, V. (1991) Beam Transformations and Nontransformed Beams. Optics Communications, 83, 123-135.

[25] Poynting vector - Wikipedia

[26] Haus, Hermann A. (1984). Waves and fields in optoelectronics. Englewood Cliffs, NJ :Prentice-Hall.

[27] Barnett, S. & Allen, L. (2010). Orbital angular momentum and nonparaxial light beams. Opt. Commun. 110. 670-678. doi: 10.1016/0030-4018(94)90269-0.

[28] Cohen-Tannoudji, C., J. Dupont-Roc, and G. Grynberg (1989), Photons and. Atoms, Introduction to Quantum Electrodynamics, John Wiley & Sons,. New York.

[29] Lax, Melvin; Louisell, William H.; McKnight, William B. (1975). From Maxwell to paraxial wave optics. Physical Review A, 11(4), 1365-1370. doi: 10.1103/PhysRevA.11.1365

[30] Berry, Michael V.; Soskin, Marat S. (1998). SPIE Proceedings., International Conference on Singular Optics - Paraxial beams of spinning light., 3487(), 6-11. doi: 10.1117/12.317704

[31] Zettili N. (2009). Quantum mechanics : concepts and applications (2nd ed.). Wiley.

[32] Classical electromagnetism and special relativity - Wikipedia

[33] Thomas precession - wikipedia

[34] Nonholonomic system - Wikipedia

[35] Parallel transport and curvature - Utah State University

[36] Angular momentum, Geometric phase and spin orbit interaction of Light by Nirmalya Ghosh - ICTS

[37] Ross, J. N. (1984). The rotation of the polarization in low birefringence monomode optical fibres due to geometric effects. Opt Quant Electron 16, 455-461. doi: 10.1007/BF00619638

[38] Bliokh, K. Y. (2009). Geometrodynamics of polarized light: Berry phase and spin Hall effect in a gradient-index medium. Journal of Optics A: Pure and Applied Optics, 11(9), 094009-. doi: 10.1088/1464-4258/11/9/094009

[39] Bliokh, K. Y.; Rodríguez-Fortuño, F. J.; Nori, F.; Zayats, A. V. (2015). Spin-orbit interactions of light. Nature Photonics, 9(12), 796-808. doi: 10.1038/nphoton.2015.201

[40] Chyba, T. H.; Wang, L. J.; Mandel, L.; Simon, R. (1988). Measurement of the Pancharatnam phase for a light beam. Optics Letters, 13(7), 562-0. doi: 10.1364/OL.13.000562

[41] Bliokh, K., Aiello, A., & Alonso, M. (2012). Spin-orbit interactions of light in isotropic media. In D. Andrews & M. Babiker (Eds.), The Angular Momentum of Light (pp. 174-245). Cambridge: Cambridge University Press. doi: 10.1017/CBO9780511795213.009

[42] Marrucci, L.; Manzo, C.; Paparo, D. (2006). Optical Spin-to-Orbital Angular Momentum Conversion in Inhomogeneous Anisotropic Media. Physical Review Letters, 96(16), 163905-. doi: 10.1103/PhysRevLett.96.163905

[43] Yao, A.M., and Padgett, M.J. (2011), "Orbital angular momentum: origins, behavior and applications," Adv. Opt. Photon. 3, 161-204, doi: 10.1364/AOP.3.000161

[44] Diffractive Optical Elements - Lens Design: OPTI 517 University of Arizona

[45] Beijersbergen, M.W.; Coerwinkel, R.P.C.; Kristensen, M.; Woerdman, J.P. (1994). Helical-wavefront laser beams produced with a spiral phaseplate. , 112(5-6), 321-327. doi: 10.1016/0030-4018(94)90638-6

The End